From the Radiologic Pathology Archives[1]

Adrenal Tumors and Tumor-like Conditions in the Adult: Radiologic-Pathologic Correlation[2]

Grant E. Lattin, Jr, MD
Eric D. Sturgill, MD
Charles A. Tujo, MD
Jamie Marko, MD
Katherine W. Sanchez-Maldonado, MS
William D. Craig, MD
Ernest E. Lack, MD

Abbreviations: ACA = adrenal cortical adenoma, ACC = adrenal cortical carcinoma, ACH = adrenal cortical hyperplasia, ACTH = adrenocorticotropic hormone, EAP = extra-adrenal paraganglioma, FDG = fluoro-2-deoxy-D-glucose, H-E = hematoxylin-eosin, IVC = inferior vena cava, MIBG = metaiodobenzylguanidine

RadioGraphics 2014; 34:805–829

Published online 10.1148/rg.343130127

Content Codes: CT GU MR OI

[1]Supported by the American Institute for Radiologic Pathology (AIRP), the Joint Pathology Center (JPC), and Uniformed Services University of the Health Sciences (USU).

[2]From the Department of Radiology and Radiological Sciences, F. Edward Hébert School of Medicine, Uniformed Services University of the Health Sciences, 4301 Jones Bridge Rd, Bethesda, MD 20814 (G.E.L., C.A.T., J.M., W.D.C.); American Institute for Radiologic Pathology, Silver Spring, Md (G.E.L., E.D.S., W.D.C.); Department of Radiology, Naval Medical Center Portsmouth, Portsmouth, Va (E.D.S.); Department of Radiology, David Grant USAF Medical Center, Travis AFB, Calif (C.A.T.); Department of Radiology, Walter Reed National Military Medical Center, Bethesda, Md (J.M.); School of Medicine, Georgetown University, Washington, DC (K.W.S.); Department of Radiology, Suburban Hospital, Bethesda, Md (W.D.C.); and Department of Endocrine Pathology, The Joint Pathology Center, Silver Spring, Md (E.E.L.). Received November 12, 2013; revision requested February 18, 2014, and received February 28; accepted March 3. For this journal-based SA-CME activity, the authors, editor, and reviewers have no financial relationships to disclose. **Address correspondence to** G.E.L. (e-mail: *grant.lattin@usuhs.edu*).

The opinions and assertions contained herein are the private views of the authors and are not to be construed as official or as representing the views of the Departments of the Army, Navy, Air Force, or Defense.

SA-CME LEARNING OBJECTIVES

After completing this journal-based SA-CME activity, participants will be able to:

- Discuss the clinical presentation and imaging spectrum of both benign and malignant adrenal tumors and tumor-like conditions in the adult.
- Describe key clinical and imaging findings in multiple benign and malignant tumors of the adult adrenal with pathologic correlation.
- Summarize diagnosis, treatment options, and prognosis for these tumors.

See www.rsna.org/education/search/RG.

Advanced imaging often reveals adrenal tumors and tumor-like conditions in both symptomatic and asymptomatic patients. When adrenal disease is clinically suspected, cross-sectional imaging can be helpful in evaluating the etiology of the patient's symptoms. When adrenal disease is incidentally identified, what the clinician and patient really want to know is whether the findings are benign or malignant, as this ultimately will affect their next step in management. Using radiologic-pathologic correlation, we broadly classify common, uncommon, and rare tumors and tumor-like conditions that can occur in the adrenal as benign or malignant. This classification follows predominant trends in observed biologic behavior while acknowledging those tumors that may behave in the minority in an unpredictable manner. We review the clinical background and presentation of functional adrenal tumors including Conn syndrome, Cushing syndrome, and catecholamine-secreting tumors, as well as their relationship with adrenal anatomy. We discuss a variety of benign tumors, including adrenal cortical adenoma (including oncocytoma) and pheochromocytoma, as well as uncommonly and rarely encountered tumors such as myelolipoma, hemangioma, lymphangioma, schwannoma, ganglioneuroma, and adenomatoid tumor. A variety of tumefactive but nonneoplastic lesions are addressed, including adrenal cortical hyperplasia, adrenal hemorrhage, adrenal cysts, and infections. Malignant tumors discussed include adrenal cortical carcinoma, the rare malignant pheochromocytoma, lymphoma, metastases, and sarcomas. For each tumor and tumor-like lesion, the clinical presentation, epidemiology, key imaging findings, diagnostic differential considerations, and management options are briefly addressed. Finally, an approach to the workup of suspected or incidentally discovered tumors is presented based on a selected literature survey and our clinical experience. Radiologists play an important role in identification and diagnosis of adrenal tumors and tumor-like conditions in both symptomatic and asymptomatic patients.

Introduction

Conditions affecting the adrenals are commonly identified at cross-sectional imaging in the adult patient population. Sometimes these lesions are clinically suspected, but more often they are incidentalomas (ie, adrenal masses discovered during diagnostic testing for another condition), which represent tumors or tumor-like conditions that a radiologist will initially assess, categorize, and potentially

TEACHING POINTS
See last page

diagnose, thus influencing the trajectory of clinical management. These tumors, in symptomatic as well as in asymptomatic individuals, may be classified in many ways, according to size, anatomic site of origin, endocrinologic signature, morphologic features, or biologic behavior. We have opted to classify the tumors and tumor-like lesions in this article according to the latter schema, as do our pathology colleagues, placing lesions into benign or malignant categories according to their predominant behaviors, as we believe that this ultimately answers the question that referring clinicians and patients seek.

Clinical Background and Endocrine Syndromes

Findings from abdominal computed tomographic (CT) studies suggest that the prevalence of adrenal incidentalomas is approximately 5% (1). Only a small number of adrenal tumors are functional and an even smaller number are malignant (2). It is important to consider that the majority of adrenal lesions are clinically silent when recommending follow-up imaging of asymptomatic patients. How to best perform follow-up for these masses is controversial and varies by medical specialty (3). Recent imaging guidelines suggest that incidentalomas with imaging features diagnostic of a benign mass (eg, myelolipoma, small cyst, adenoma) require no additional workup or follow-up imaging, and that stability at imaging of an adrenal mass for 12 months makes a benign diagnosis most likely (3,4).

Most incidentally discovered adrenal tumors are nonfunctional and benign, with fewer than 10% having detectable endocrine functionality and fewer than 5% being malignant (5). Some diseases of adrenal origin may not require imaging for initial clinical recognition, but imaging almost always plays an important role during disease workup in confirming the etiology.

Conn Syndrome

Aldosterone-secreting adrenal cortical adenoma (aldosteronoma) accounts for up to 2% of all unanticipated adrenal masses (2). Conn syndrome, or primary aldosteronism due to an adrenal cortical adenoma (ACA), has classically been characterized clinically by hypertension and hypokalemia. However, it has become increasingly recognized that most patients with primary aldosteronism do not have hypokalemia (6). The more common causes of primary aldosteronism include bilateral idiopathic adrenal cortical hyperplasia (ACH) (~60% of cases) and an aldosterone-secreting ACA (~35%), with unilateral adrenal hyperplasia and other rarer causes accounting for the remainder of cases (6). Plasma aldosterone-to-renin ratio is the diagnostic test of choice.

Cushing Syndrome

Between 2% and 15% of ACAs produce cortisol (2). Hypercortisolism can result in Cushing syndrome, which is characterized by symptoms such as weight gain and deposition of adipose tissue (especially in the face, neck, or back), hypertension, easy bruisability, amenorrhea, hirsutism, acne, muscle weakness, diabetes, and mood changes. Noniatrogenic hypercortisolism resulting in Cushing syndrome may be pituitary dependent (Cushing disease) (~60%–70% of cases in adults) with the remaining cases being pituitary independent (7). Pituitary-independent causes include ectopic adrenocorticotropic hormone (ACTH) production, rarely ectopic corticotropic-releasing factor (CRF) secretion, primary pigmented nodular adrenocortical disease (PPNAD), and macronodular hyperplasia with marked adrenal enlargement (MHMAE). Cushing syndrome caused by an adrenal adenoma is classified as an ACTH-independent form of hypercortisolism. ACAs causing Cushing syndrome are often >2 cm in size and readily visualized with CT or MR imaging (8). Preclinical or subclinical Cushing syndrome occurs when a patient has a cortisol-secreting tumor, but steroid secretion is insufficient to elicit classic signs or symptoms of the syndrome.

Increased Catecholamines

The reported frequency of pheochromocytoma among adrenal masses is variable, ranging from 1.5% to 23%, with the actual prevalence likely being near 3%–6% (3). The widespread use of CT and magnetic resonance (MR) imaging is allowing more pheochromocytomas to be detected before the patient presumably becomes symptomatic, although not all patients become symptomatic, with increasing numbers of unanticipated pheochromocytomas being discovered at imaging performed for unrelated symptoms (9). In symptomatic patients, pheochromocytomas release catecholamines, which may lead to a classic triad of symptoms consisting of episodic headache, sweating, and tachycardia, with or without hypertension that may be paroxysmal or sustained. Other symptoms include palpitations, tremor, pallor, and dyspnea. The diagnosis is usually established with a 24-hour urine measurement of fractionated catecholamines and metanephrines.

Virilization and Feminization

Clinically recognizable signs and symptoms associated with virilization and feminization in the

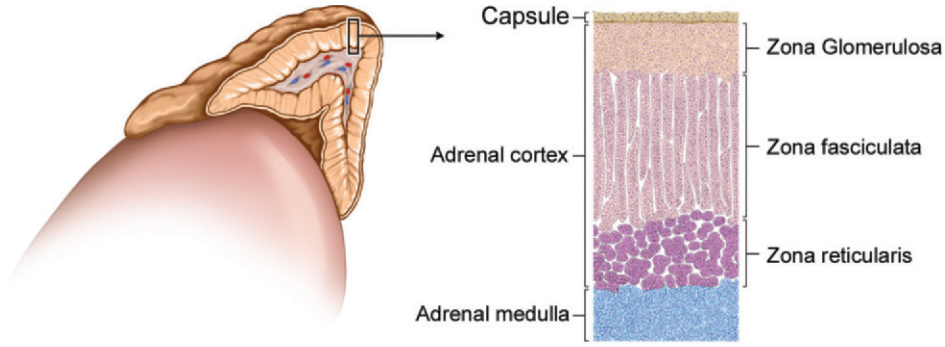

Figure 1. Normal adrenal anatomy. Drawing of the adrenal in transverse section shows the three layers of the adrenal cortex and inner medulla.

adult patient such as male-pattern baldness, hirsutism, clitoromegaly, and gynecomastia, are usually associated with adrenal cortical tumors and have a higher prevalence of malignancy (7).

Normal Anatomy of the Adrenals

The adrenals are paired endocrine glands that sit anterosuperior and slightly medial to the upper pole of each kidney. They are responsible for hormone production and release, and thus play a crucial role in regulation of metabolism, salt and water balance, response to stress, and sexual functioning. Each adrenal is a bipartite structure with cortex and medulla having different embryogenesis, structure, and function.

The outer cortex typically envelops the medulla and is made up of three zones, each one producing a different class of corticosteroids: the outermost zona glomerulosa lies just beneath the adrenal capsule and produces mineralocorticoids, the middle zona fasiculata produces glucocorticoids, and the inner zona reticularis produces sex steroids or gonadocorticoids. The inner medulla is composed of chromaffin cells that are arranged in nests or sheets and produce catecholamines, both epinephrine and norepinephrine with epinephrine predominating (Fig 1). Chromaffin cells are typically concentrated in the head (inferomedial) and body (central) of the gland.

Because the adrenals are responsible for the production of hormones that play a role in systemic functions, they are highly vascularized to allow dissemination of their products. Three arterial sources supply the adrenals: the superior, middle, and inferior suprarenal arteries. These branches originate from the inferior phrenic arteries, abdominal aorta, and renal arteries, respectively. The venous drainage of each adrenal is via a single vein that then empties into the left renal vein or inferior phrenic vein on the left, and directly into the inferior vena cava (IVC) on the right.

Benign Tumors and Tumor-like Conditions

Adrenal Cortical Adenoma

Adrenal cortical adenoma (ACA) is the most common tumor of the adrenal. While the true prevalence is not known exactly, estimates range from 1.4% to 8.9% based on autopsy series, with the prevalence increasing with age (10).

ACA is typically a well-circumscribed encapsulated solid mass that is yellow on cross-sectioning due to abundant neutral lipid content (Fig 2). Atypical gross appearances include a dark brown or black color, the so-called black adenoma, as well as intratumoral hemorrhage and cystic changes (Fig 2). At histopathologic examination, tumor cells have abundant pale-staining lipid-rich cytoplasm, which is often arranged in short cords or nests. A relatively rich and delicate vascular supply is present. These findings of lipid-rich cells and an abundant vascular network account for the classic imaging features seen on cross-sectional views of the tumor (11) (Fig 2).

While ultrasonography (US) is not considered the first-line imaging modality for suspected adrenal tumors or tumor-like lesions, lesions of the adrenal can be found incidentally during abdominal or retroperitoneal US examinations. At US, ACAs appear as well-circumscribed, slightly heterogeneous mixed echogenicity round or oval lesions (12).

At CT, ACAs are usually well-marginated lesions of uniform attenuation. The characteristic low attenuation of ACAs depends predominantly on the amount of intracytoplasmic lipid. Studies have shown that using a cutoff value of 10 HU or less at unenhanced CT has high sensitivity (79%) and specificity (96%) for an ACA (13,14). The majority of ACAs have enough lipid content to be accurately diagnosed; the remaining 10%–40% of tumors, the so-called "lipid-poor" ACAs, will have higher attenuation values at unenhanced CT (13) and would be considered indeterminate.

Figure 2. ACA in a 53-year-old woman with a history of diabetes and hypertension. **(a)** Axial T1-weighted in-phase MR image shows a hypointense left adrenal mass (arrowhead) with mild heterogeneity. **(b)** Axial T1-weighted out-of-phase MR image shows a marked decrease in signal intensity (arrowhead) in the posterior aspect of the mass, confirming the presence of an increased intravoxel fat-to-water ratio. **(c)** Photograph of a gross specimen of a partially encapsulated left ACA shows cystic change and old hemorrhage (white arrowhead) along with fresh hemorrhage (black arrowhead). **(d)** Photomicrograph (original magnification, ×100; hematoxylin-eosin [H-E] stain) of the same ACA as in **c** shows lipid-rich cells (black arrowheads) with rounded nuclei and inconspicuous nucleoli. Also evident is the rich vascular supply, with multiple small vessels (white arrowheads) throughout the tumor.

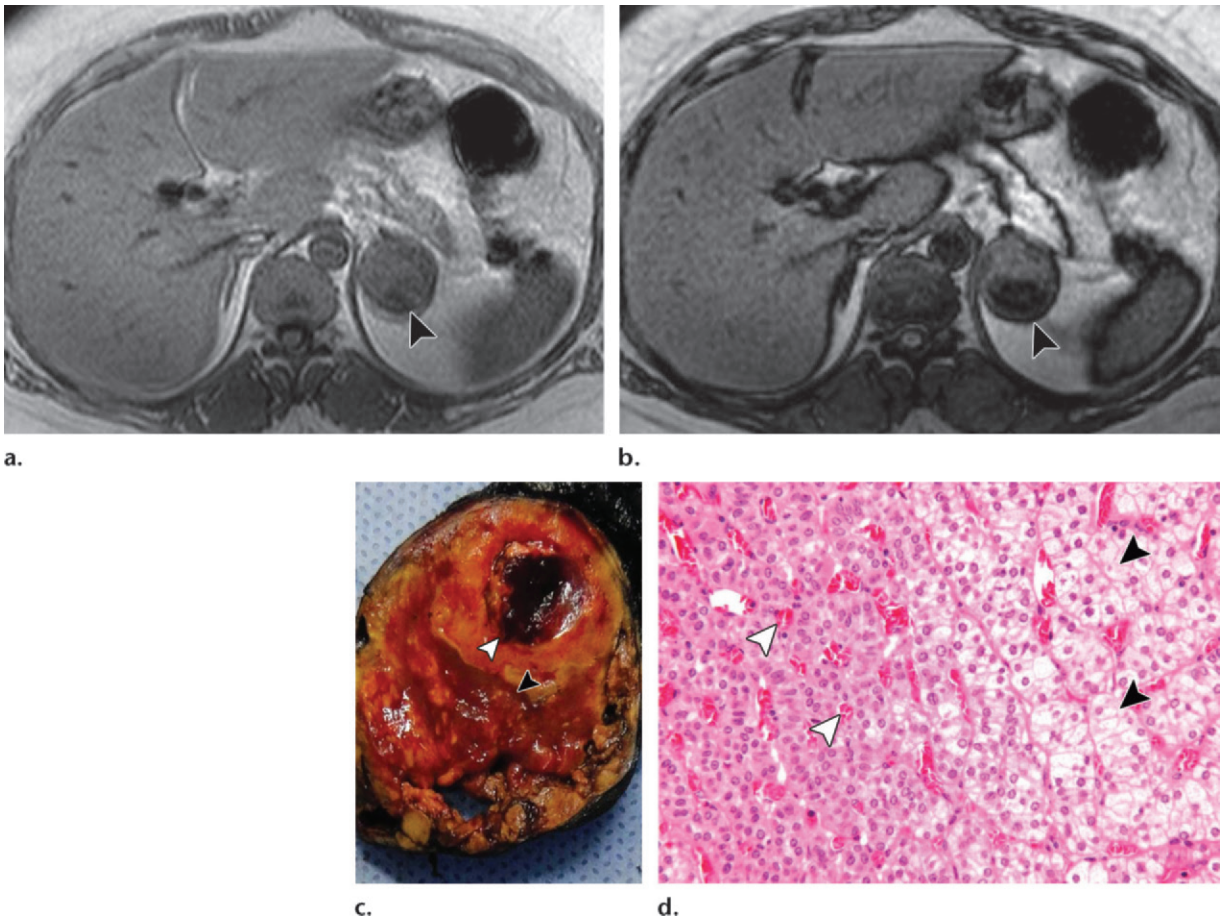

Subsequent studies have shown that washout criteria are helpful in characterizing many of the lipid-poor ACAs and excluding more concerning lesions at CT. The concept of washout relates to the inherent rich vascularity of ACAs, and the tendency for these tumors to not retain contrast material for extended time periods, as opposed to malignant adrenal tumors. Washout values can be calculated using a few different methods, with most centers obtaining nonenhanced images, early enhanced images (usually at either 1 minute or in the portal venous phase), and delayed enhanced images (at 15 minutes). Calculation of the absolute and relative washout percentages is performed using attenuation values from regions of interest (ROI) placed on the lesion at the different phases of contrast enhancement.

Formulas generally used to calculate washout values are as follows: Absolute washout = {[early enhanced CT (HU) − delayed CT (HU)]/[enhanced CT (HU) − unenhanced CT (HU)]} × 100%. Relative washout = {[early enhanced CT (HU) − delayed CT (HU)]/[early enhanced CT (HU)]} × 100%. Absolute and relative washout values of greater than 60% and 40%, respectively, allow fairly confident diagnosis of adenoma, with sensitivity ranging from 88% to 96% and specificity ranging from 96% to 100% (13–16).

Teaching Point

MR chemical shift imaging exploits the different precessional frequencies of protons in water versus protons in fat within the same voxel and creates in-phase and out-of-phase images in which signal from the protons is either additive or subtractive from one another. As with unenhanced CT, this sequence takes advantage of the abundant intracytoplasmic lipid found in the majority of ACAs. Most adenomas show a significant decrease in signal intensity on the out-of-phase images (17,18) (Fig 2).

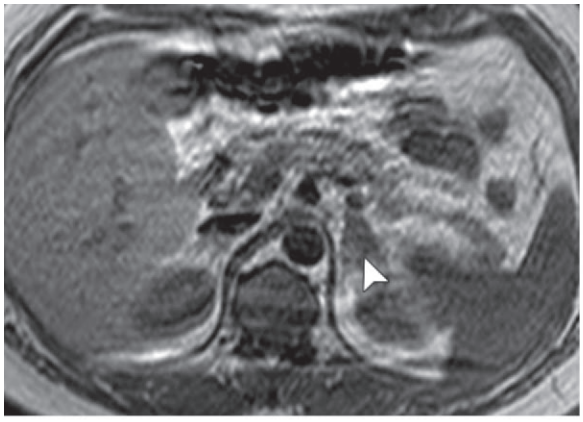

a.

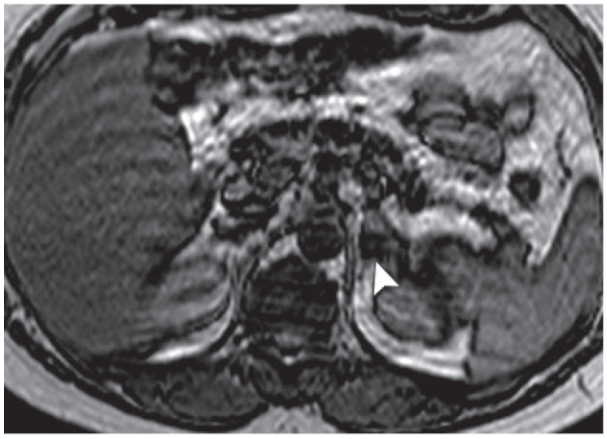

b.

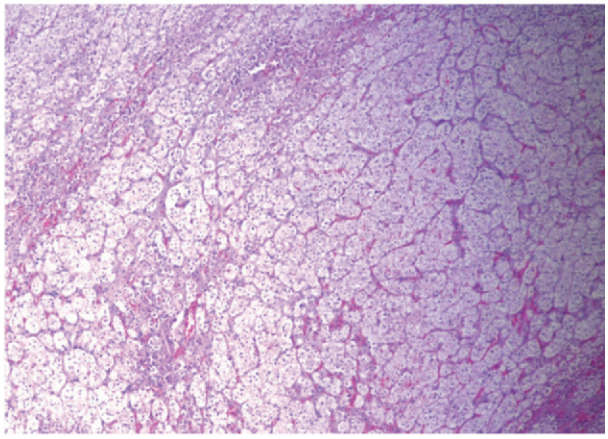

c.

Figure 3. ACH in a 33-year-old man with multi–drug-resistant arterial hypertension and hypokalemia due to unilateral nodular cortical hyperplasia. **(a)** Preoperative axial T1-weighted in-phase MR image shows a small, homogeneous, intermediate signal left adrenal mass (arrowhead). **(b)** Preoperative axial T1-weighted out-of-phase MR image shows a significant drop in signal intensity (arrowhead), consistent with the presence of intracytoplasmic fat, underscoring the radiologic overlap that can occur in the spectrum of adrenal cortical nodular hyperplasia and ACA. **(c)** Photomicrograph (original magnification, ×100; H-E stain) of the left adrenal shows rare unilateral nodular cortical hyperplasia.

The appearance of ACAs at cross-sectional imaging may overlap with those of other benign and malignant lesions, including pheochromocytomas, metastases, and small adrenal cortical carcinomas (ACCs). While size less than 3 cm can help predict which lesions are more likely to be benign, it cannot be reliably used alone (15). The presence of lipid, detected with CT or MR imaging, is not 100% specific for ACAs, as metastatic clear cell renal cell carcinoma, pheochromocytoma, and ACC can contain lipid (1,13–15,18,19). Although lipid in ACAs is most often microscopic fat (identified by loss of signal intensity from in-phase to out-of-phase imaging), rarely larger aggregates of adipocytes are present (macroscopic fat), as may be seen in lipomatous or myelolipomatous metaplasia. In addition, pheochromocytomas have been documented meeting washout criteria similar to those of ACAs at three-phase contrast-enhanced CT (including a 15-minute delay), with 25%, 29%, and 33% of pheochromocytomas meeting relative, absolute, or either (relative or absolute) washout criteria, respectively (19). Atypical appearances of ACAs include changes relating to intralesional cystic degeneration or less often hemorrhage, thus making accurate imaging diagnosis more challenging.

Despite these limitations, a small (<3 cm) homogeneous lesion that measures less than 10 HU at nonenhanced CT is, for practical purposes, an ACA unless there are compelling clinical factors (eg, coexistent renal clear cell carcinoma) to suggest otherwise. In addition, when an adrenal mass measuring up to 4 cm is identified at "routine" contrast-enhanced CT in a patient without a known history or current evidence of malignancy, the mass is statistically still likely to be an adenoma (4).

Treatment guidelines have been developed by various international endocrinologic societies and often include biochemical evaluation for adrenal hyperfunction, with treatment relying on either medical management (eg, idiopathic Conn syndrome without identifiable tumor) or adrenalectomy, depending on the clinical scenario. Most incidentally identified ACAs, especially in older patients without a known malignancy, have no implications for the patient's further management.

Adrenal Cortical Hyperplasia

Based on a review of autopsy series of approximately 35,000 subjects, the prevalence of ACH is estimated to be 0.51%, increasing with age (20). Hyperplasia can manifest as either a diffuse

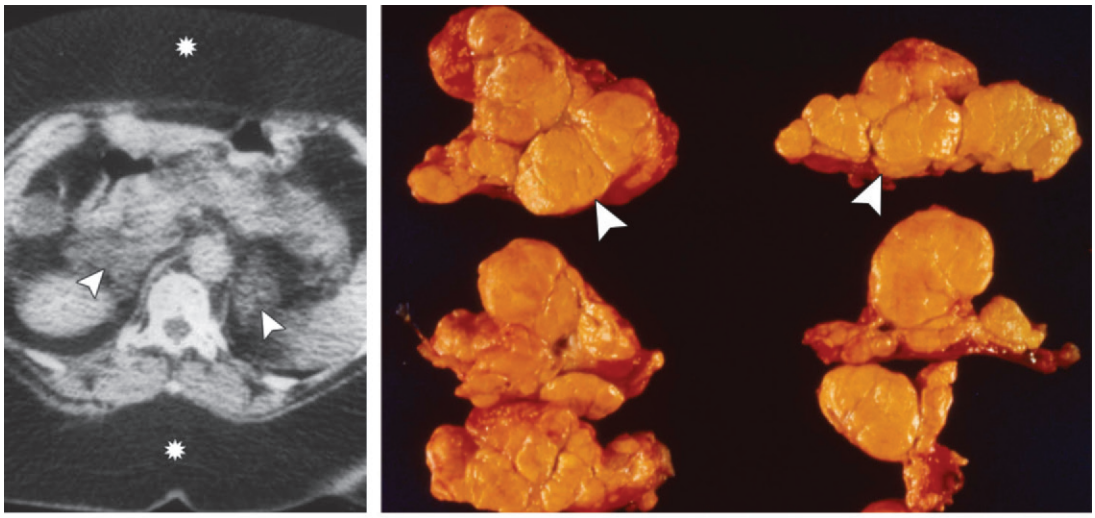

Figure 4. ACTH-independent Cushing syndrome due to macronodular hyperplasia with marked adrenal enlargement (MHMAE) in a 46-year-old woman. **(a)** Preoperative axial contrast-enhanced CT image shows bilateral hypo- to isoattenuating macronodules (arrowheads) throughout both adrenals. Also notice the marked abdominal subcutaneous fat deposition (stars) due to the Cushing syndrome. **(b)** Photograph of sectioned bilateral adrenalectomy gross specimens shows multiple yellow to tan macronodules (arrowheads) replacing the adrenal cortex in a patient with confirmed adrenal cortical nodular hyperplasia. The adrenals weighed >100 grams combined.

process involving the entire adrenal(s) or as nodular hyperplasia. Nodular hyperplasia is usually multifocal and bilateral, also increasing in prevalence with age. In a series of 113 consecutive adult necropsies, the adrenals were examined histologically and 35% were described as normal, 50% as having mild nodularity, and the remainder as having distinct nodularity (21). The average age of patients with distinct nodularity was 65 years versus 50 years for the normal group. This study demonstrated that an increasingly nodular appearance of the adrenal can occur with age (21).

These nodules are composed of variably-sized groups of lipid-rich cells, some of which can show exuberant growth with nodular or diffuse architecture with impingement on the medulla (Fig 3). Hyperplasia is sometimes characterized as micro- versus macronodular in appearance, depending on whether the nodules are visible with the unaided eye at gross examination. In some patients with ACA, histologic evaluation of the adrenal may show smaller hyperplastic cortical micronodules that are present in the attached cortex (21). This suggests that some nonfunctional ACAs may in fact be larger, dominant hyperplastic cortical nodules (Fig 3) (21). Since this article is focused on adrenal conditions in the adult, congenital adrenal hyperplasia, a condition seen more commonly in childhood, is not discussed.

The clinical presentation of ACH can often overlap with that of hyperfunctioning ACAs. If the hyperplastic adrenal cortex is actively producing hormones, pituitary- or ACTH-independent Cushing syndrome or hyperaldosteronism can occur (7). Diffuse ACH usually manifests as smooth to slightly lobular thickening of the entire adrenal, maintaining its overall normal inverted-V or inverted-Y appearance (22,23). Rarer causes of diffuse ACH with adrenal enlargement may include ectopic ACTH production (and very rare cases of ectopic corticotropic-releasing factor production) (7).

Nodular ACH can be identified at cross-sectional imaging if the nodules are large enough (eg, macronodular). At CT, nodular ACH can appear as more focal hypo- to isoattenuating nodules on the background of more normal adrenal tissue, or the intervening cortex can appear atrophic. There are two distinct rare types of nodular hyperplasia that are also associated with pituitary-independent Cushing syndrome. Macronodular hyperplasia with marked adrenal enlargement (MHMAE), also known as adrenocorticotropin-independent macronodular adrenal hyperplasia (AIMAH), can result in marked enlargement and distortion of the adrenals, with multiple bulging yellow nodules at gross pathologic analysis (Fig 4). Primary pigmented nodular adrenocortical disease (PPNAD) is characterized by normal to slightly enlarged adrenals that contain small pigmented nodules, with atrophy of the intervening cortex. PPNAD can be seen in association with Carney complex, which is a rare disorder consisting of cardiac and cutaneous myxomas, mucocutaneous pigmentation, as well as other tumors (7).

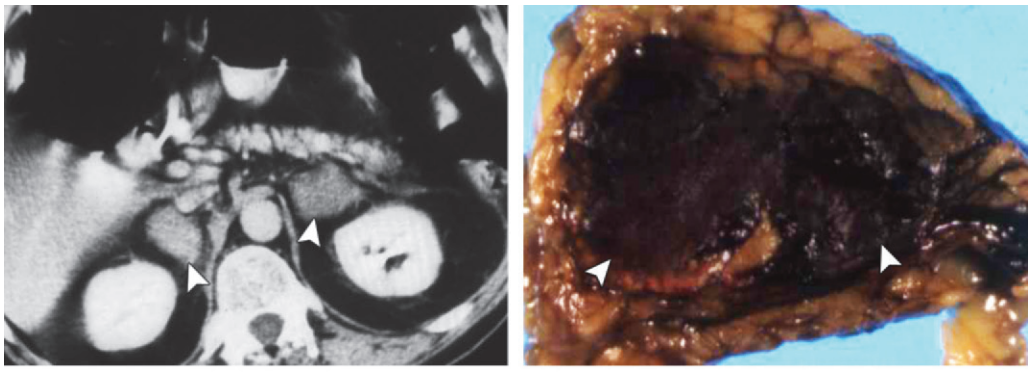

a. b.

Figure 5. Adrenal hemorrhage in a 62-year-old man hospitalized for severe brain infarction with upper gastrointestinal bleeding during his hospital course. **(a)** Axial postcontrast CT image shows bilateral homogeneously hyperattenuating adrenal enlargement (arrowheads), consistent with hemorrhage. **(b)** Postmortem photograph of an adrenal gross specimen shows marked fresh hemorrhage (arrowheads) throughout the gland, centered in the medulla.

Treatment of ACH varies greatly according to the clinical manifestations associated with hormone excess. ACH in the absence of clinical or biochemical evidence of adrenal cortical hyperfunction is not treated. It is important to remember that adrenal venous sampling is essential in directing therapy for symptomatic patients, as there is not always concordance with the cross-sectional imaging findings (6). This is especially true in older patients, who may have cortical nodules associated with age, as seen at CT, intermingled with hormone-producing ACH or an ACA. In patients with primary aldosteronism due to an aldosterone-producing ACA or unilateral hyperplasia, laparoscopic unilateral adrenalectomy is the preferred treatment, with normalization of serum potassium and return to a normotensive state in a significant number of cases. Bilateral idiopathic hyperplasia in the setting of primary aldosteronism is treated medically, relying on a mineralocorticoid receptor blocker such as spironolactone, in addition to sodium intake restriction and lifestyle modification (6).

Adrenal Hemorrhage

Teaching Point

Adrenal hemorrhage in the adult can be broadly divided into traumatic and nontraumatic causes, with the former accounting for the majority of cases (24). Traumatic adrenal hemorrhage is most commonly seen in the setting of blunt trauma, with multiple other coexistent visceral injuries often identified (25). The prevalence of traumatic hemorrhage has been shown to be as high as 26%, based on an early series of autopsies of 50 patients who died after severe abdominal or thoracic injury (26). More recent studies have shown that approximately 2% of patients undergoing abdominal and pelvic CT for trauma have evidence of adrenal hemorrhage (25–27).

Posttraumatic adrenal hemorrhage is usually unilateral, although bilateral involvement can occur (25). While uncommon overall, nontraumatic adrenal hemorrhage is typically bilateral and can be caused by a wide range of conditions, with the most common being stress, hemorrhagic diathesis or coagulopathy, or an underlying adrenal mass (24,28) (Fig 5). One series of 2000 consecutive autopsies performed over an 8-year period yielded an overall prevalence of 1.8% for bilateral adrenal hemorrhage in a nontrauma setting (28).

Common stress events include severe burns, sepsis, surgery, or hypotension. Anticoagulant therapy can cause spontaneous adrenal hemorrhage (29). Causes of adrenal vein thrombosis, including hypercoagulable states, can cause hemorrhagic infarction of the gland (29,30). ACAs, myelolipomas, pheochromocytomas, metastases, and ACC are some of the adrenal masses known to cause spontaneous adrenal hemorrhage, therefore careful inspection is required at imaging to exclude such lesions when adrenal hemorrhage is identified. Follow-up cross-sectional imaging may be warranted, as the underlying mass may not be apparent at the initial imaging examination.

Adrenal hemorrhage is not usually clinically apparent and is more often an unanticipated finding at imaging or autopsy. Symptoms can range from mild flank or back pain to shock-like symptoms, depending on the degree of hemorrhage. Acute adrenal insufficiency is rare, even in the case of bilateral adrenal hemorrhage, and can manifest as hypotension, hyponatremia, and hyperkalemia (24–28).

At gross inspection, adrenal hemorrhage can range from punctate 1–3-mm regions of dark red and brown discoloration in an otherwise normal gland to a massively enlarged and distended gland, filled with hemorrhagic debris, up to 15

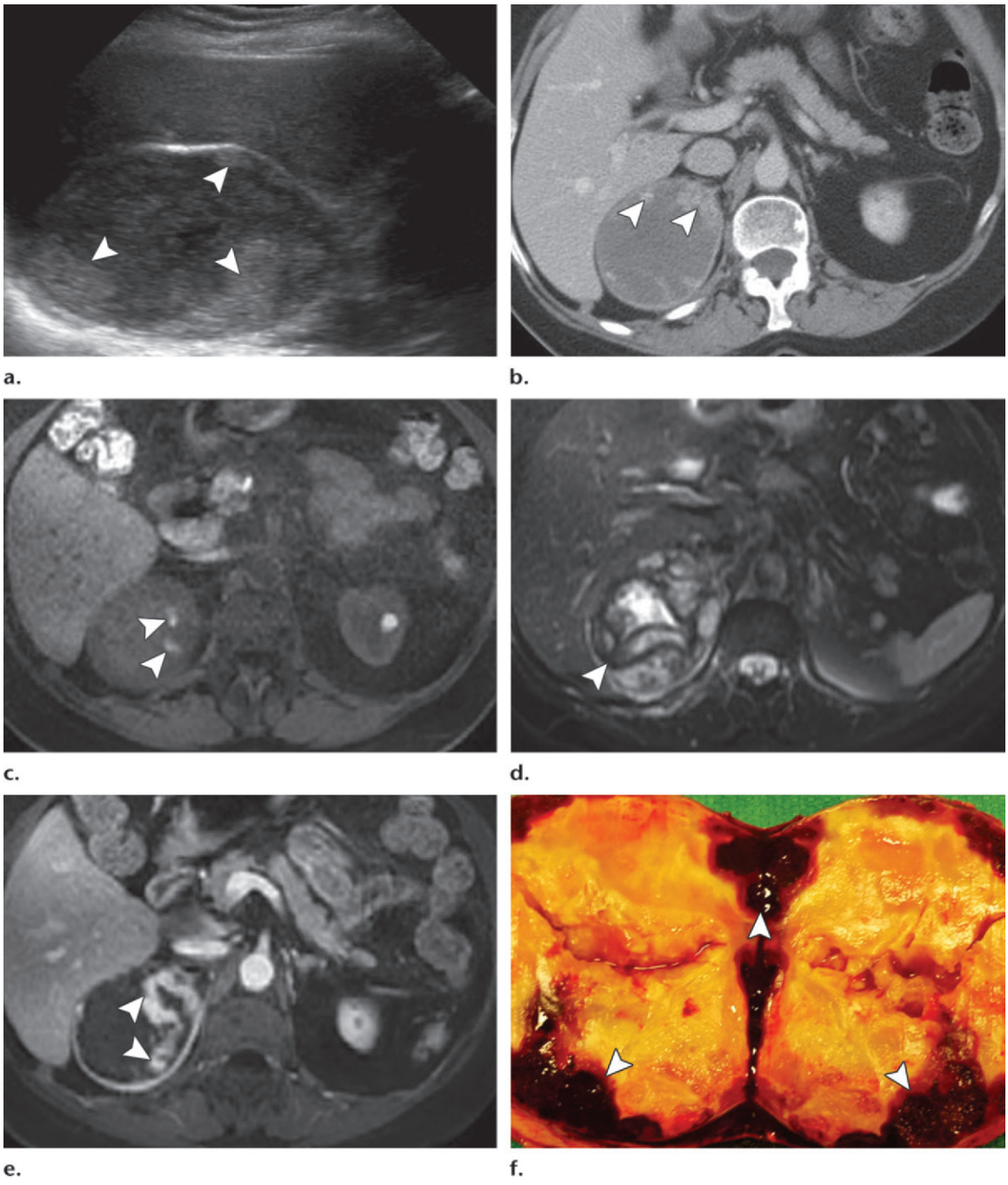

Figure 6. Adrenal hemorrhage in a 72-year-old woman with hypertension controlled with two medications and a known stable 2.3-cm right adrenal mass, most consistent with an adenoma. Imaging performed 10 years later showed interval enlargement to 8 cm with a workup that was negative for any evidence of stress, trauma, anticoagulation, infection, or urine metanephrines. Postresection pathologic analysis confirmed an organizing hematoma. Given the size of the hematoma, it was not conclusive whether the bleeding was from the adenoma or other possible causes. **(a)** Sonographic image shows a well-circumscribed suprarenal mass with heterogeneous echotexture characterized by peripherally hyperechoic areas (arrowheads). **(b)** Axial postcontrast CT image shows heterogeneously decreased attenuation centrally with peripherally enhancing areas (arrowheads). **(c)** Axial precontrast fat-saturated T1-weighted MR image shows areas of increased signal intensity correlating with recent hemorrhage (arrowheads). **(d)** Axial fat-saturated T2-weighted MR image shows heterogeneous signal centrally, consisting of areas of hyperintensity correlating with intermediate-period hemorrhage and linear hypointensity likely representing areas of hemosiderin and fibrin (arrowhead). **(e)** Axial postcontrast fat-saturated T1-weighted MR image shows areas of avid enhancement peripherally (arrowheads) correlating with recent hemorrhage. **(f)** Photograph of the bivalved gross specimen shows an organizing hematoma (pale yellow areas) with regions of fresh hemorrhage (arrowheads).

cm in diameter. Hemorrhage most often affects the medulla with variable degrees of cortical involvement (Fig 5). Extension of hemorrhage through the cortex can be seen both histologically and at imaging. In cases of traumatic adrenal hemorrhage, the right adrenal is more commonly affected. This has been attributed to compression of the right adrenal between the liver and spine and transmission of elevated venous pressure from the IVC through the short draining adrenal vein on the right side (26–28).

Imaging appearances of adrenal hemorrhage have been well described in the literature. At US, more acute hemorrhage appears as a solid, heterogeneously hyperechoic lesion without associated internal vascularity (Fig 6). As the hematoma matures, the central portions become more hypoechoic, and over time the area assumes more of a cyst-like appearance—anechoic with possible peripheral curvilinear hyperechoic calcifications. Gradual decrease in size is expected in the absence of repeated hemorrhage.

At CT, most cases of adrenal hemorrhage appear round or oval, with attenuation depending on the acuity of the hemorrhage (Fig 6). A less common appearance of adrenal hemorrhage includes extensive suprarenal hemorrhage that obliterates the gland entirely (27). More recent hemorrhage will appear relatively hyperattenuating, with attenuation values ranging from 50 to 90 HU at unenhanced CT. Over time, the size and attenuation values will decrease and the majority will become undetectable. Calcification can occur and may be the only residual imaging evidence of a prior hemorrhage that has otherwise resolved.

As with US and CT, the appearance of adrenal hemorrhage at MR imaging depends on the age and composition of the blood products. Early hemorrhage is isointense on T1-weighted images and hypointense on T2-weighted images. In the intermediate period, the paramagnetic effects of methemoglobin dominate, causing hyperintensity on both T1- and T2-weighted images (Fig 6). Eventually, hemosiderin and a fibrous capsule result in a T1- and T2-hypointense rim with a variable degree of susceptibility artifact on gradient-echo images (18,24,25).

In the setting of nontraumatic hemorrhage, the primary differential diagnostic considerations are an underlying mass that has spontaneously bled, including, as noted earlier, ACA, pheochromocytoma, myelolipoma, and a hypervascular metastasis. Identifying a small mass that has caused the bleeding can be challenging, especially at initial presentation. Clinical history, such as symptoms of adrenergic overactivity in the setting of pheochromocytoma, can help narrow the differential diagnosis. Identifying macroscopic fat can strongly suggest an underlying myelolipoma. Serial imaging can be helpful to assess for the evolution of a hematoma, as described earlier. Alternatively, contrast-enhanced MR imaging using subtraction sequences can be used to more effectively detect underlying enhancing lesions in an otherwise heterogeneous adrenal hemorrhage.

Since most adrenal hemorrhages spontaneously resolve, treatment is usually supportive. In the presence of large bilateral adrenal hemorrhage, clinical suspicion should remain high for acute adrenal insufficiency, which is fatal if left untreated. In that case, treatment includes prompt glucocorticoid administration with concomitant intravenous saline therapy. Immediate mineralocorticoid administration is not necessary as long as the dosage of glucocorticoid is high enough (>50 mg of hydrocortisone daily) to activate mineralocorticoid receptors (31).

Adrenal Cysts

Overall, adrenal cysts are relatively rare, with a reported prevalence of 0.06% based on autopsy series (32). Clinical presentation can range from a silent lesion that is incidentally detected at imaging to flank or abdominal pain due to mass effect (32,33). Females are more commonly affected than males by a 2:1 to 3:1 ratio, with most presenting in the 3rd to 5th decade of life (32). There is no predilection for the right versus left gland, and bilateral cysts are present in approximately 15% of cases (34). These cysts can range in size from less than a centimeter to greater than 20 cm (32–34), although most are small to medium-sized, with one recent study reporting median and mean baseline sizes of 4.2 cm and 5.3 cm, respectively (35).

Adrenal cysts are a heterogeneous group of disorders and, as such, various classification schemes have been proposed and subsequently modified over the years. Currently, these cysts are classified into four categories: vascular or endothelial cysts, pseudocysts, simple (true) cysts, and parasitic cysts. Together, pseudocysts and endothelial cysts represent greater than 80% of all adrenal cysts (34). There is growing data, including electron microscopy and immunohistochemical studies, supporting the theory that both pseudocysts and endothelial cysts may be variants of vascular adrenal cysts (32). Simple (true) cysts are relatively uncommon. Parasitic cysts are rare and usually secondary to *Echinococcus granulosus* infection (32,34).

At gross inspection, adrenal cysts are well-circumscribed, encapsulated lesions. Pseudocysts have a thicker wall compared with thin-walled endothelial and epithelial cysts. Internally, pseudocysts are typically unilocular and contain blood

and amorphous yellow-brown material, whereas endothelial cysts are multilocular and contain serous, serosanguinous, or pale fluid (Fig 7). At histopathologic examination, the wall of a pseudocyst contains dense, hyalinized material with occasional calcification or osseous metaplasia. Adrenal cortical cells can be found in the wall of pseudocysts. Endothelial cysts are lined by cells that resemble normal endothelium. Simple (true) cysts are unilocular with a simple epithelial lining. Parasitic cysts have variable internal complexity depending on the stage of infection, from purely cystic components to more complex contents including daughter vesicles, freed scolices, and brood capsules (the so-called "hydatid sand") (32,33).

Adrenal cysts can be detected at abdominal radiography, which may demonstrate inferior displacement of the ipsilateral kidney (33). US often demonstrates a well-circumscribed hypoechoic to anechoic lesion with a thin wall, typically measuring less than 3.5 mm, especially in endothelial and epithelial cysts, while pseudocysts may have a slightly thicker cyst wall (32,34). Internal scattered echogenicity, debris, or fluid-fluid levels suggest more recent hemorrhage into a pseudocyst (34).

CT of an uncomplicated adrenal cyst usually shows a well-circumscribed, nonenhancing, hypoattenuating lesion with internal attenuation of less than 20 HU and a thin wall (Fig 7) (34). Increased internal attenuation suggests hemorrhage or debris. Calcifications may be peripheral (mural), scattered throughout the lesion, or central in location (rarely) and have been reported in 15%–30% of adrenal vascular cysts (32). Peripheral calcification is seen more often with pseudocysts and parasitic cysts, while septal calcification can be present in endothelial cysts (Fig 7) (34).

MR imaging of uncomplicated adrenal cysts shows a well-circumscribed, thin-walled, centrally nonenhancing lesion with internal uniform hypointensity on T1-weighted images and hyperintensity on T2-weighted images (18). The presence of T1 hyperintense signal is usually secondary to hemorrhage within the cyst (18). The imaging appearance of an echinococcal adrenal cyst depends on the stage of infection (36). Possible findings include a simple cyst, a multilocular lesion with internal septa, focal rounded internal daughter vesicles, the "water lily" sign, and septal or mural calcifications (34,36). The presence of extra-adrenal foci of *Echinococcus* (ie, hydatid disease) is important in making a confident diagnosis of echinococcal adrenal cysts, since isolated adrenal involvement is exceedingly rare (36).

Differential diagnostic considerations for a predominantly cystic adrenal lesion include both benign and malignant lesions. ACA, hemangioma, pheochromocytoma, ACC, and metastatic disease can have varying degrees of a cystic appearance at imaging. Detailed imaging evaluation is required to detect findings suggesting an underlying neoplasm. Worrisome findings include an irregular

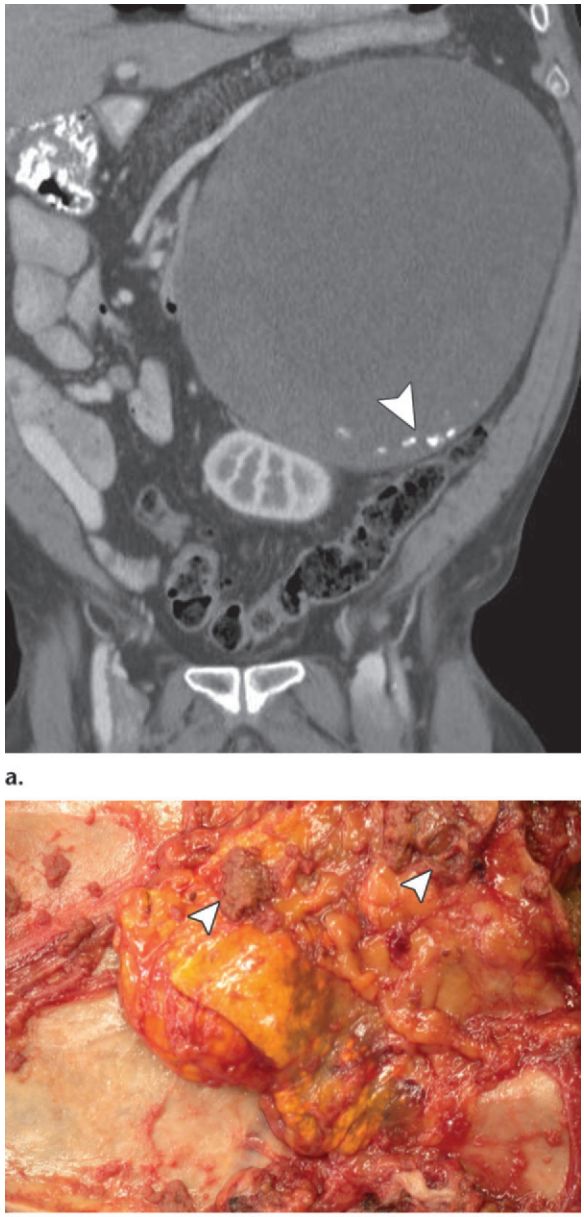

a.

b.

Figure 7. Adrenal cyst in a 67-year-old man with a large left retroperitoneal pseudocyst and subsequent adrenal cortical insufficiency after removal. **(a)** Coronal postcontrast CT image shows a predominantly hypoattenuating well-circumscribed mass with dystrophic calcification (arrowhead) within the wall, displacing the left kidney inferiorly. **(b)** Photograph of the surgical gross specimen shows red-tan friable tissue consistent with internal hemorrhage (arrowheads). The cyst wall ranged from 2 to 30 mm in thickness. This degree of cyst wall thickening correlated with an underlying adrenal cortical functional adenoma with subclinical Cushing syndrome.

Figure 8. Adrenal myelolipoma in a 37-year-old man. Axial postcontrast CT image shows an incidental left adrenal mass containing macroscopic fat (arrowhead), which is highly consistent with a myelolipoma.

thick wall (>5 mm), mural or septal nodular enhancement, or any degree of internal enhancement suggesting a solid component (34,37).

Management and treatment algorithms for adrenal cysts vary and are controversial, due to the overall rarity of such lesions and the difficulty in establishing a preoperative pathologic diagnosis (38). Some advocate resection for all cysts, while others resect only lesions considered at increased risk of hemorrhage or secondary complications. Proposed resection criteria include cysts greater than 5 cm (due to risk of hemorrhage), all functional symptomatic cysts, or cysts with imaging characteristics that do not safely exclude underlying malignancy (eg, enhancing soft-tissue components) (38). These criteria are reflected more so in the surgical literature describing removal of clinically significant lesions, possibly explaining differences from other committee consensus recommendations that consider resection of incidental adrenal masses measuring >4 cm (4,39).

Recent imaging literature regarding the natural history of adrenal cysts suggests that the features of benign adrenal cysts include a smooth, thin wall measuring ≤ 3 mm, fluid attenuation (0–20 HU), and minimal complicated features (thin septa and wall calcifications), with interval increase in cyst size being frequently observed (60% of cases) (35). This tendency for a benign adrenal cyst to increase in size over time should not be misinterpreted as indicative of an underlying malignancy or secondary complication when observed as an isolated finding (35).

Myelolipoma

Adrenal myelolipoma is a benign tumor of varied composition of adipose tissue and myelopoietic cells, usually trilinear elements. Myelolipoma is relatively uncommon, occurring in 0.08%–0.2% of cases in autopsy series (40). These tumors are not hormonally active and usually are asymptomatic, unless they grow to a large size and exert mass effect or have internal hemorrhage. Very rarely, myelolipomatous foci are associated with adrenal functional disorders such as Cushing syndrome (41).

Teaching Point

Myelolipomas contain gross fat and are characteristically identified at CT based on the presence of macroscopic fat (Fig 8). In one series, the average nonenhanced CT attenuation value was –74 HU, with approximately 24% of isolated adrenal myelolipomas containing calcification (41). At MR imaging, myelolipomas follow characteristics of fat, with increased signal intensity on T1-weighted images and signal dropout on fat-saturated T2-weighted images.

In general, macroscopic fat-containing adrenal lesions are myelolipomas. Rarely, mimics may include ACC or large adrenal cysts with peripherally entrapped fat. Very rarely, additional mimics may include ACA with lipomatous metaplasia, adrenal lipoma, or adrenal teratoma. Size measuring greater than 7 cm has been proposed as a threshold for removal due to mass effect and increased risk of hemorrhage (42). Long-standing or poorly treated congenital adrenal hyperplasia has been associated with development of massive bilateral myelolipomas (7).

Pheochromocytoma

The World Health Organization (WHO) reserves the term *pheochromocytoma* for adrenal medullary paraganglioma or tumors arising from chromaffin cells in the adrenal medulla. Closely related tumors in extra-adrenal sympathetic and parasympathetic paraganglia are classified as extra-adrenal paragangliomas (EAPs). Pheochromocytomas typically secrete both norepinephrine and epinephrine, but norepinephrine is usually the predominant catecholamine. The exact incidence of pheochromocytoma is unknown, but it is estimated to occur in 2–8 cases per 1 million people per year (43). Classically, the vast majority of patients with pheochromocytomas were thought to be symptomatic. However, as more patients undergo cross-sectional imaging for unrelated reasons, the number of pheochromocytomas identified in otherwise asymptomatic patients continues to increase, with reported clinical, imaging, and autopsy occurrence rates as high as 10%–17%, 57.6%, and 76%, respectively (9,43).

Symptoms are often due to adrenergic excess, and the diagnosis is supported by elevated levels of circulating or excreted catecholamines and metabolites (7). At gross examination, the tumors are usually well-circumscribed masses ranging in size

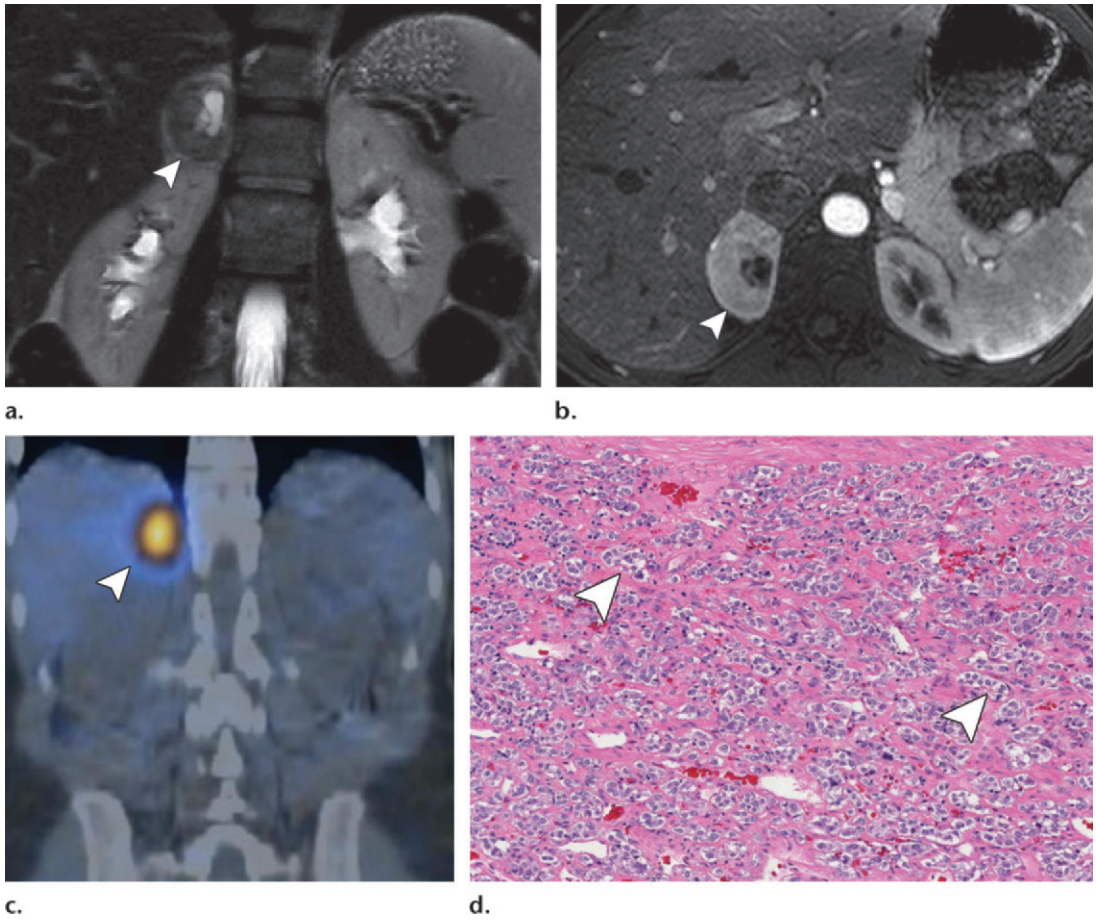

Figure 9. Adrenal pheochromocytoma in a 46-year-old woman with poorly controlled hypertension and ventricular tachycardia due to the pheochromocytoma. **(a)** Coronal T2-weighted MR image shows a right adrenal pheochromocytoma (arrowhead) with heterogeneous signal intensity and focal areas of cystic change. **(b)** Axial postcontrast T1-weighted MR image shows avid enhancement in the arterial phase (arrowhead). **(c)** Coronal fused CT/MIBG (metaiodobenzylguanidine) image shows focal intense radiotracer uptake in the adrenal mass (arrowhead), confirming the diagnosis. **(d)** Photomicrograph (original magnification, ×100; H-E stain) of a pheochromocytoma shows a nesting microscopic pattern (arrowheads).

from 3–5 cm (7). Pheochromocytomas are typically firm and gray-white and may have areas of central degenerative changes including fibrosis or cystic change. At microscopic examination, architectural patterns include a combination of alveolar (nesting) and trabecular (36% of cases), predominantly alveolar (35%) (also referred to as nesting), and predominantly trabecular (27%) (44) (Fig 9). Cytoplasm can be eosinophilic and finely granular but may range from amphophilic to basophilic. Some nuclei may contain "pseudoinclusions" representing invaginations of cell cytoplasm within folds of the nuclear membrane.

Hereditary syndromes associated with pheochromocytomas and EAPs include multiple endocrine neoplasia (MEN) syndrome types 2A and 2B, neurofibromatosis type 1 (NF-1), von Hippel–Lindau disease (VHL), and familial paraganglioma syndrome (PGL), as outlined in the Table (13,45). These syndromes are associated with germline mutations that activate the *RET* gene (MEN), inactivate the *NF-1* gene (NF-1), inactivate the *VHL* gene (VHL), and inactivate the genes for succinate dehydrogenase (SDH) subunits B, C, or D (PGL) (46). Problematically, the well-recognized syndromes associated with these mutations may be clinically silent. Thus, many neuroendocrine tumors previously thought to be sporadic (due to an absence of syndromic stigmata) harbor underlying mutations. One group of researchers has identified these clinically silent mutations in up to 25% of patients with pheochromocytomas; a second group believes the percentage of pheochromocytomas and EAPs with an underlying genetic basis is close to 30% (47,48).

Either CT or MR imaging is the first-line modality for characterizing and localizing suspected pheochromocytoma. Tumors are typically round or oval masses of similar attenuation to the surrounding soft-tissue structures at unenhanced imaging, with a reported mean attenuation of 35.9 HU ± 9.8 (49). Scattered, often

Hereditary Syndromes Associated with Pheochromocytomas and EAPs

Syndrome	Risk of Tumor (%)	Mutated Gene
Multiple endocrine neoplasia (proto-oncogene)	50	RET
Neurofibromatosis 1	1	NF-1
von Hippel–Lindau disease	10–20	VHL
Familial paraganglioma syndrome	20 (estimated)	SDHB, SDHC, SDHD

Note.—Adapted and reprinted, with permission, from reference 45.

punctate calcifications can be seen in up to 10% of cases (50). Lesions usually measure 3–5 cm in diameter but range from 1 to 10 cm or more. Regardless of lesion size, radiologic evaluation of pheochromocytoma is complicated by varying degrees of lesion degeneration, necrosis, calcification, fibrosis, cystic change, and intracellular lipid degeneration, creating imaging appearances that often overlap with other diagnoses such as degenerating ACAs and metastases (51,52). Further complicating features include the tumor's inconsistent washout features, which cannot be relied on to differentiate pheochromocytoma from other adrenal lesions, particularly ACAs (19).

At MR imaging, the classic homogeneously "light bulb"–bright T2 lesion is infrequently encountered and accounts for as few as 11% of cases (53). In truth, the majority of homogeneous lesions are less bright than cerebrospinal fluid and tend to match the spleen in signal intensity. Unfortunately, no histologic features have been found to explain these patterns, to our knowledge (54). The lesions may be homo- or heterogeneous (Fig 9), depending on internal components of fibrosis, necrosis, hemorrhage, and cyst formation. In a relatively recent article, the most commonly observed pattern (39%) was a heterogeneous enhancing lesion with multiple high-signal-intensity pockets or cysts as evidenced by areas of T2 prolongation (53) (Fig 9). Pheochromocytoma's broad range of imaging features has earned it the nickname "an imaging chameleon" (55). Radiologists are reminded to include pheochromocytoma in the differential diagnosis of low-attenuation adrenal lesions, lesions with avid washout, and lesions with a dominant cystic component, depending on the clinical scenario and laboratory findings.

Teaching Point

Many different radionuclide agents are available for imaging pheochromocytomas and EAPs. These agents are typically employed when clinically suspected tumors cannot be localized or confirmed with standard cross-sectional imaging. Furthermore, they are of benefit in certain cases where there is a need to exclude bilaterality, multifocal disease, metastatic disease, or postoperative recurrence.

^{131}I- or ^{123}I-labeled metaiodobenzylguanidine (MIBG) is a norepinepherine analog that was specifically developed for use as a neuroendocrine agent. With a specificity that approaches 100% and a sensitivity that ranges from 79% to 88%, MIBG is considered by many to be the nuclear agent of choice for detecting sympathoadrenal paragangliomas (56) (Fig 9).

An alternative uptake mechanism can be found in fluoro-2-deoxy-D-glucose (FDG) positron emission tomography (PET), which relies on cellular proliferation and metabolism, as opposed to sympathetic differentiation and somatostatin receptor expression. In an older review, the overall sensitivity of FDG PET for intra- and extra-adrenal paragangliomas was 72% (57), with a more recent study documenting a sensitivity of 78% for localizing nonmetastatic paraganglioma (58). When specifically targeting known metastatic disease from malignant SDHB (succinate dehydrogenase subunit B)–associated pheochromocytomas and paragangliomas, the sensitivity of FDG PET approached 100% (59). It must be noted that while FDG PET is sensitive, FDG remains a nonspecific agent accumulated by multiple other lesions including non–paraganglioma-related metastatic disease, ACCs, and ACAs.

Less frequently used PET agents, such as fluorodopamine and hydroxyephedrine, have also been used successfully to identify pheochromocytoma. These agents take advantage of selective uptake by sympathoneuronal structures, rapid background clearance, and near-immediate visualization of abnormalities (60).

Although treatment often begins with pharmacologic blockade, the ultimate goal is cure with complete tumor resection. For this reason, the radiologist is critical in preoperative assessment of disease localization, which can be complicated by both multifocality and metastases.

No imaging feature of the primary lesion can reliably distinguish the more common benign pheochromocytoma from the rare malignant neoplasm unless there is evidence of direct local extension into the surrounding structures (liver,

kidney, pancreas) or distant metastases (eg, bone, lymph nodes, liver, or lung) (11,55). Regional lymph nodes are the most frequent location for metastatic deposits, followed by the axial skeleton, liver, lung, and kidney (11). Local invasion into the surrounding fat and feeding vessels may be identified but is not considered a definitive feature of malignancy, since tumors that lack this feature have been known to metastasize (11). The definition of malignancy rigorously relies on identification of metastases in locations where chromaffin cells are not otherwise found, to eliminate the possibility of misclassifying multicentric primary lesions as metastases or as development of loco-regional recurrence (7).

Hemangioma

Adrenal hemangiomas are rare, with a prevalence of 1 per 10,000 autopsies, and are typically asymptomatic due to their size, measuring <2 cm (7). Those discovered at imaging often leading to surgery are much larger, measuring >10 cm (Fig 10).

Hemangiomas consist of two main types, capillary and cavernous, with the latter group being more frequent and demonstrating dilated vascular spaces and delicate septa in a more spacious pattern under the microscope. These tumors are primarily vasoformative neoplasms that tend to be highly vascular. CT shows these tumors to be well-demarcated with hypoattenuation or heterogeneous attenuation (61) (Fig 10). Phleboliths are characteristic, although more irregular calcifications may also be present (Fig 10).

Postcontrast cross-sectional imaging displays peripheral discontinuous nodular enhancement with or without delayed central filling (Fig 10). At MR imaging, the tumor typically is hypointense on T1-weighted images and hyperintense on T2-weighted images, although there may be T1-weighted variability with areas of increased signal intensity due to hemorrhage or necrosis (22). Image-guided biopsy or resection is performed, when needed, to confirm benignity.

Lymphangioma

Adrenal lymphangioma is an exceedingly rare tumor usually discovered incidentally. This benign tumor has a prevalence estimated at 0.06%, is typically asymptomatic, and may occur at any age with a peak in the 3rd to 6th decades of life (62). Previous case reports may have classified some of these tumors as adenomatoid tumors or as lymphangiomatous endothelial cysts occurring in the adrenal.

The gross appearance of adrenal lymphangioma is similar to that of those occurring elsewhere in the body, namely a multilocular cyst containing clear fluid that sometimes may be blood-tinged. Histologically, these tumors have a cystic or cavernous architecture and contain proteinaceous fluid and scattered lymphocytes with interstitial lymphoid aggregates. Immunohistochemistry for D2-40 may aid in identifying the lining of lymphatic vessels.

Figure 10. Adrenal hemangioma in an 84-year-old woman with progressive left flank pain. Coronal postcontrast CT image shows a cavernous adrenal hemangioma with well-circumscribed margins and capsular calcifications that demonstrates peripheral nodular discontinuous enhancement (arrowhead).

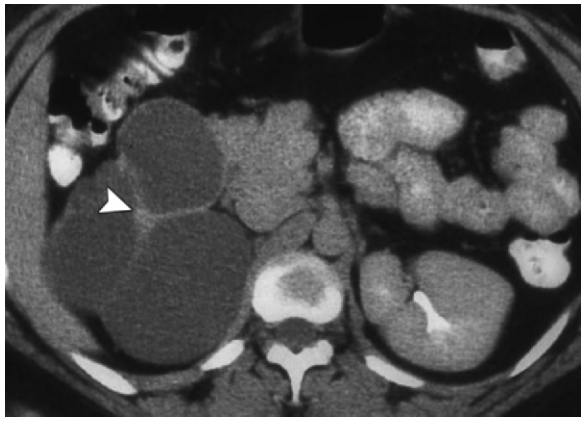

Figure 11. Adrenal lymphangioma in a 35-year-old woman with flank pain. Axial postcontrast delayed phase CT image shows a right adrenal lymphangioma, characterized by a few enhancing septa (arrowhead) surrounding locules of hypoattenuating simple fluid.

CT demonstrates a hypoattenuating, thin-walled cystic lesion without internal enhancement that is at or near fluid attenuation (Fig 11). Enhancement of the cyst wall or thin septa is identified (Fig 11). MR imaging features are consistent with a fluid-containing cyst, characterized by decreased signal intensity on T1-weighted images and increased intensity on T2-weighted images (18).

The differential diagnosis may include an adrenal cyst, hemangioma, cystic pheochromocytoma, or schwannoma with cystic degeneration. A multilocular cyst with thin septa and CT attenuation of simple fluid is most suggestive of a lymphangioma.

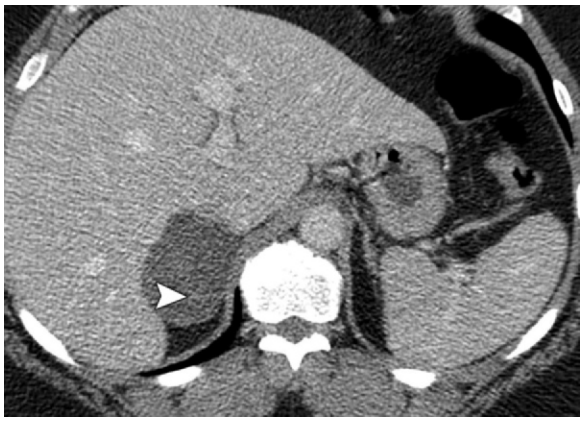

Figure 12. Adrenal schwannoma in a 46-year-old man with right flank pain. Axial postcontrast CT image shows subtle heterogeneous enhancement (arrowhead) in a hypoattenuating right adrenal mass, which was shown to be a schwannoma.

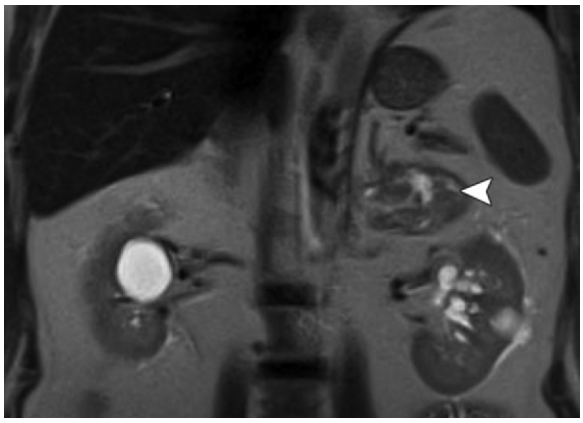

Figure 13. Ganglioneuroma in a 69-year-old man in whom previous CT for diverticulitis showed an incidental 6-cm left adrenal ganglioneuroma. Coronal T2-weighted MR image shows that the mass has heterogeneously increased signal intensity with a whorled appearance (arrowhead).

However, features such as unilocular morphology, hemorrhage, or soft-tissue enhancement may suggest an alternative diagnosis. Treatment is surgical when warranted.

Schwannoma

Schwannomas are benign nerve sheath tumors of neural crest origin that uncommonly occur in the retroperitoneum (3%) and are rarely observed in the adrenal (63). These lesions are typically benign, although malignant cases do exist and are usually associated with neurofibromatosis type 1. This tumor may affect any age group and has an equal gender distribution; it has a predilection for adults 20–40 years of age (64).

Although often discovered incidentally, adrenal schwannomas may manifest with abdominal pain. The typical schwannoma is encapsulated, giving a well-circumscribed margin. Histologically, schwannomas often have a combination of Antoni A and B patterns with intense S-100 positivity. The term *ancient schwannoma* is used for those tumors that have marked degenerative change, which may include old hemorrhage, calcification, cystic change, and nuclear atypia.

A schwannoma appears as a heterogeneously enhancing hypoattenuating mass at CT (Fig 12). T1-weighted images demonstrate isointense signal to muscle with hyperintensity on T2-weighted images, but MR imaging features are nonspecific, as there may be marked variability depending on the degree of degenerative change (63). As a result, the differential diagnosis for adrenal schwannoma includes pheochromocytoma and malignant tumors. Complete excision is the treatment of choice.

Ganglioneuroma

Neuroblastoma, ganglioneuroblastoma, and ganglioneuroma can all be observed in adults, although the former two are much more common in children. Consequently, our discussion focuses on ganglioneuroma, which is more commonly seen in young adults. Ganglioneuroma is a benign neurogenic tumor arising along the sympathoadrenal axis; it is more frequent in the posterior mediastinum and retroperitoneum than in the adrenal medulla (20%–30% of cases) (64). At gross examination, ganglioneuroma is a firm, well-circumscribed tumor with an average size of about 8 cm and has a gray-white to tan-yellow appearance at cross-sectioning.

Nonenhanced CT features include decreased attenuation measuring <40 HU with punctate or discrete calcification (65). Contrast-enhanced CT shows a homogeneously hypoattenuating mass as compared with muscle, which surrounds vessels rather than narrowing or occluding them (66). At MR imaging, decreased signal intensity on T1-weighted images and heterogeneously increased signal intensity on T2-weighted images are observed, with gradual delayed enhancement (Fig 13). The hyperintensity seen on T2-weighted images may have a whorled appearance (65) (Fig 13).

The differential diagnosis includes many benign and malignant tumors, including neuroblastoma and ganglioneuroblastoma in younger patients, as well as ACA, pheochromocytoma, and ACC. Complete excision is the preferred treatment.

Adenomatoid Tumor

Adenomatoid tumor of the adrenal is a rare, benign tumor of mesothelial origin. Fewer than 40 primary tumors have been reported in the adrenal, with a male predilection and an age range of 24–64

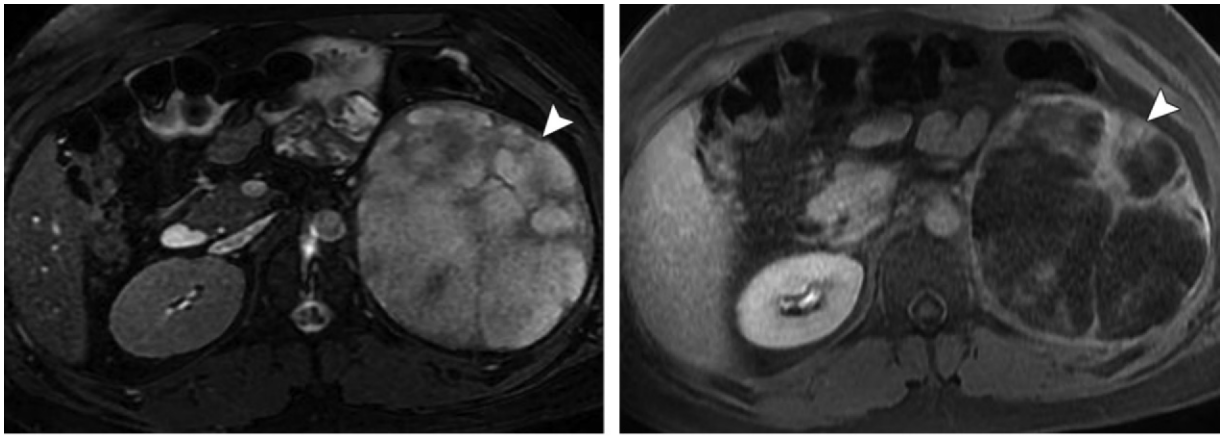

a. b.

Figure 14. Adenomatoid tumor in a 22-year-old man with right lower quadrant pain and an incidental left adrenal mass noted at imaging, which was subsequently resected and confirmed to be an adenomatoid tumor. **(a)** Axial fat-saturated T2-weighted MR image shows a well-circumscribed solid and cystic 18-cm mass (arrowhead) with heterogeneous signal intensity. **(b)** Axial postcontrast T1-weighted MR image shows heterogeneous enhancement of the solid components (arrowhead).

years of age. Typically, these tumors are seen on the left side more often than the right and may be incidentally discovered, although pain and hematuria have been reported (67) (Fig 14).

Pathologic features include a smooth, gray-white, homogeneous tumor that microscopically has sieve-like cytoplasmic vacuoles and gland-like spaces. Immunohistochemical stains for cytokeratin and calretinin are useful in confirming the mesothelial origin of this tumor (68). Dystrophic calcification and "signet ring" cells may be present. The signet ring cells may be misleading and suggest metastatic adenocarcinoma (67).

Given that these tumors can be solid and cystic, contrast-enhanced CT shows a heterogeneously hypoattenuating mass with a well-circumscribed border. Calcifications may be present. MR imaging findings are nonspecific and variable on T1-weighted, T2-weighted, and postcontrast images, so the differential diagnosis for adenomatoid tumors includes pheochromocytoma and ACC (69) (Fig 14). Surgery is the treatment of choice.

Oncocytoma

Adrenal oncocytoma is an uncommon benign tumor with about 110 cases reported in the literature and a median patient age of 46 years (70). When occurring in the adrenal, this tumor has also been referred to as oncocytic ACA or oncocytic adrenocortical neoplasm. These tumors have a slight female predilection (1.8:1), occur more frequently on the left (1.5:1), and have a mean size of about 9 cm (70). Adrenal oncocytoma is generally nonfunctioning (up to 69.5% of cases); however, in a significant minority of cases these tumors may be symptomatic due to steroid production, leading to Cushing syndrome, virilization, or feminization (71). Traditionally, malignant behavior has been thought to be rare, but at least 61 of the reported cases to date demonstrated borderline malignant potential (47) or were frankly malignant (24,72).

Gross specimens of adrenal oncocytoma appear encapsulated and are mahogany brown or dark tan at cross-sectioning. Areas of degenerative change may be present. Microscopically, tumors have abundant deeply eosinophilic (mitochondria-rich) cells (Fig 15). As with other ACAs, immunohistochemistry is typically positive for vimentin, melan A, inhibin-α, and calretinin and may be immunoreactive for synaptophysin (70) (Fig 15). They also may be immunoreactive for mitochondrial antigen MTCO2 and variably positive for CK8, CK18, and CD10 (71). The presence of one major or one minor criterion may indicate a malignant or borderline tumor, respectively. The major criteria include greater than 5 mitoses per 50 high-power fields, atypical mitoses, and venous invasion. The minor criteria include microscopic necrosis, sinusoidal invasion, capsular invasion, and size greater than 10 cm or weight greater than 200 grams (73).

Cross-sectional imaging shows a well-marginated often large mass with heterogeneous enhancement (72) (Fig 15). Unfortunately, this nonspecific appearance leads to consideration of tumors such as ACC, lymphoma, or lipid-poor myelolipoma. Generally, the lack of vascular invasion or lymphadenopathy argues against the former diagnoses. Excision is the treatment of choice regardless of biopsy results, given the size and uncertainty of biologic behavior.

Adrenal Infections

Fungal, bacterial, mycobacterial, parasitic, and viral infections can affect the adrenals. Hydatid

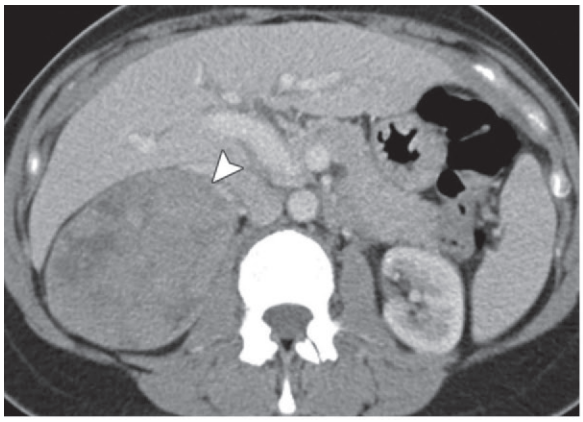

a.

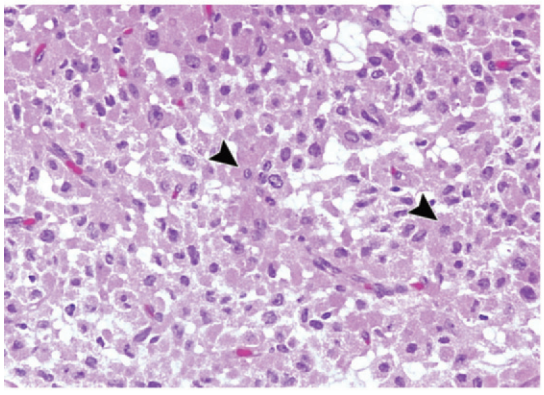

b.

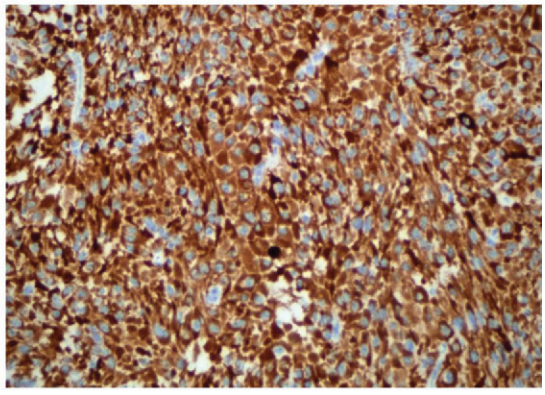

c.

Figure 15. Confirmed borderline adrenal oncocytoma in a 48-year-old woman with right flank pain and a right adrenal mass. **(a)** Axial postcontrast CT image shows a 12-cm well-demarcated heterogeneously enhancing solid mass (arrowhead). **(b)** Photomicrograph (original magnification, ×100; H-E stain) shows diffuse oncocytic cells with eosinophilic cytoplasm (arrowheads) and high nuclear grade. **(c)** Photomicrograph (original magnification, ×100; melan A stain) shows that the oncocytic cells display avid positivity, characterized by the diffuse brown color of the cytoplasm.

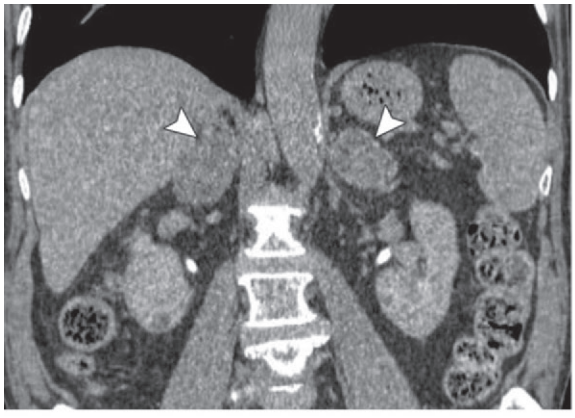

a.

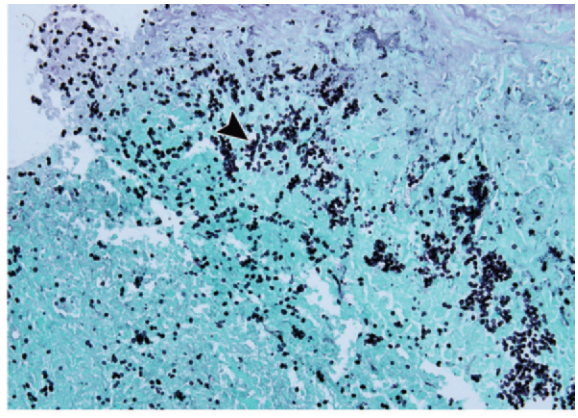

b.

Figure 16. Adrenal infection in a 73-year-old man with a 3-month history of fatigue, loss of appetite, and unexplained weight loss. **(a)** Coronal postcontrast delayed phase CT image shows symmetrically enlarged hypoattenuating adrenals (arrowheads). **(b)** Photomicrograph (original magnification, ×40; Gomori methenamine-silver [GMS] stain) of a biopsy specimen shows numerous small budding yeast (arrowhead) with morphology typical of *Histoplasma capsulatum*.

involvement generally has the classic appearance of a primary cyst with secondary cysts internally, as discussed previously. Up to 80% of patients with disseminated fungal infection have involvement of the adrenal at autopsy, with histoplasmosis and paracoccidioidomycosis being most common (7) (Fig 16). Less common infections are blastomycosis, coccidioidomycosis, and cryptococcosis. Typically, well-defined bilateral adrenal masses or enlargement is common (74) (Fig 16). Lung infection typically precedes identification of adrenal involvement.

Tuberculosis can affect both adrenals. Bilateral adrenal enlargement can occur in both tuberculosis and histoplasmosis, although the appearance may be less symmetric in the former

(22). Later, CT features in both diseases can include decreased central attenuation due to necrosis and calcifications.

Adrenal abscess formation occurs rarely and is usually unilateral. Bacteria such as *Escherichia coli*, group B *Streptococcus*, and *Bacteroides* spread hematogenously and may be associated with hemorrhage, making it difficult to exclude an underlying adrenal tumor (7). It is also important to remember that immunocompromised patients such as those with acquired immunodeficiency syndrome (AIDS) can also have cytomegalovirus (CMV) infection affecting the adrenals. At autopsy of 74 AIDS patients, the adrenals were infected with CMV in 84% (75). Rarely, these patients may present clinically with adrenal insufficiency, but the adrenal involvement with CMV is typically not identified at premortem examinations and has been described with normal-appearing adrenals at cross-sectional imaging (76).

Malignant Tumors

Adrenal Cortical Carcinoma

ACC is a rare tumor with a prevalence of 1–2 per 1 million population (77). Females are more commonly affected than males, with a female-to-male ratio approaching 1.5:1 (Fig 17). There is a biphasic age distribution, with peak incidences in early childhood and middle age (4th to 5th decades) (78). ACC may be sporadic or associated with hereditary syndromes including Li-Fraumeni syndrome, Beckwith-Wiedemann syndrome, Carney complex, congenital adrenal hyperplasia, and multiple endocrine neoplasia (MEN) type 1 (79).

The clinical presentation of ACC may be related to increased steroid production by the tumor or bulk disease causing abdominal pain, back pain, weight loss, or early satiety (80). ACCs may result in Cushing syndrome, hyperaldosteronism, or increased sex steroid production with virilization or feminization (77,78).

At gross examination, ACCs are usually bulky with an average size of about 12 cm and average weight of over 800 grams. The tumors may near completely replace the normal adrenal. At cross-sectioning, ACCs typically display yellow to red-brown discoloration and often have areas of hemorrhage and necrosis. The histopathologic criteria that are most useful in establishing the diagnosis of a malignancy include mitotic activity, capsular invasion, and permeation of vascular spaces. Cellular pleomorphism is also a common feature. The three most common histologic patterns are trabecular, nesting or alveolar, and diffuse sheet-like growth. There is no correlation between histologic pattern and functional status of the tumor (81).

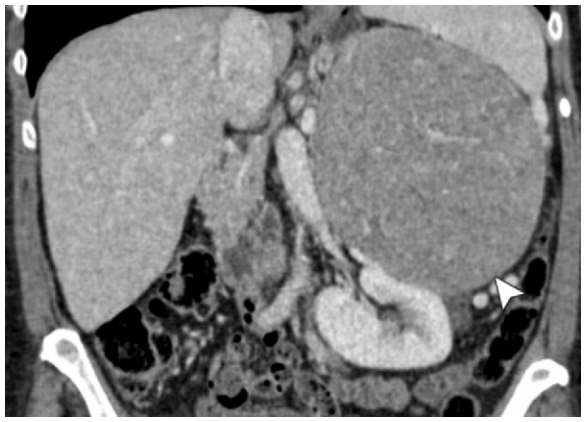

Figure 17. ACC in a 67-year-old woman with metrorrhagia, hot flashes, and breast pain; laboratory results confirmed abnormal sex hormone secretion. Coronal postcontrast CT image shows an enhancing well-circumscribed ACC (arrowhead) originating from the left suprarenal fossa, displacing the left kidney inferiorly and the spleen and left hemidiaphragm superiorly.

Immunohistochemical staining can be useful to distinguish ACC from other neoplasms such as pheochromocytoma and renal cell carcinoma. For example, ACCs are negative for chromogranin A, which is characteristically positive in tumors of the adrenal medulla. Positivity for steroidogenic factor–1 would suggest ACC over a renal neoplasm. Epithelial membrane antigen is typically negative in ACC but positive in renal malignancies. High levels of Ki-67 expression are more commonly seen with ACC than with ACA, but no standard accepted threshold for accurate differentiation of these neoplasms currently exists, to our knowledge. In recent years, authors have identified molecular genetic and chromosomal alterations that are seen in sporadic ACC. For example, loss of heterozygosity for tumor suppressor genes coding for p53, p57, and insulin-like growth factor–2 have been implicated (82).

Regardless of the modality used to image an ACC, certain features will remain consistent. For example, ACCs are typically large masses located superior to the kidney in the perirenal space of the retroperitoneum. They are primarily soft tissue and may contain areas of necrosis, hemorrhage, or calcification. Although bilateral in 10% of cases, ACC is typically unilateral with slightly more involvement of the left adrenal (53%) than the right (47%) (Fig 17) (7). Local spread into adjacent organs, regional lymph nodes, and the renal vein or IVC can be seen.

At US, ACCs are round or oblong mass lesions arising from the adrenal. The masses tend to be well-defined with lobulated contours. When small, ACC may demonstrate homogeneous echotexture. As the tumor enlarges, heterogeneous echotexture

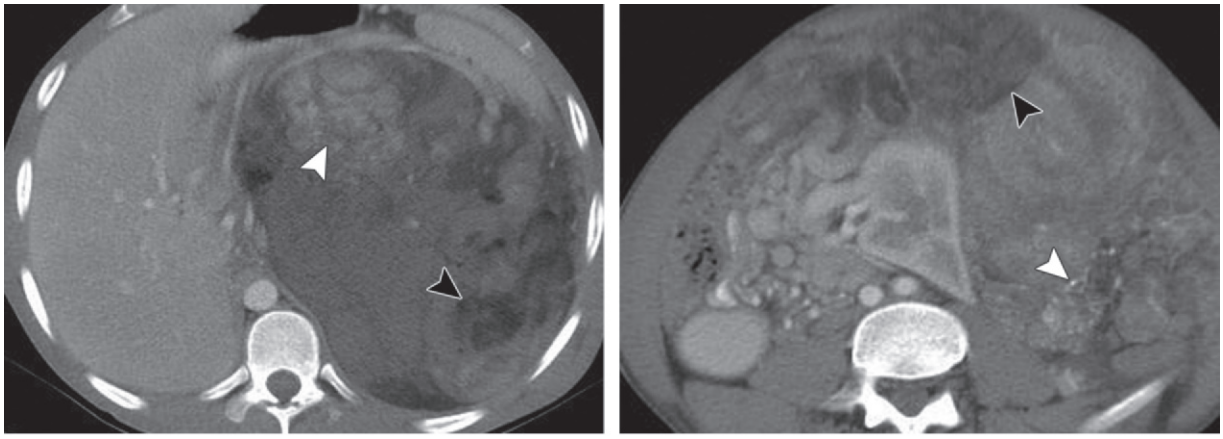

a. b.

Figure 18. ACC in a 20-year-old man with early satiety and increasing abdominal girth. **(a)** Axial postcontrast CT image shows an ACC in the left retroperitoneum with peripheral nodular soft-tissue enhancement (white arrowhead) that also contains aggregates of macroscopic fat (black arrowhead). **(b)** Axial postcontrast CT image shows inferomedial displacement of the left kidney, with punctate calcification (white arrowhead) and more fat extending anteriorly (black arrowhead).

is commonly seen due to hemorrhage and necrosis. Both hyperechoic and hypoechoic regions may be present. Echogenic foci with or without posterior acoustic shadowing due to calcification can be seen in a minority of cases. In addition, a thick echogenic capsule-like rim (which may completely or incompletely surround the mass) has been described (83).

At unenhanced CT, ACCs are large well-defined suprarenal masses with heterogeneous attenuation and a tendency to displace regional structures (84) (Fig 17). ACCs typically have nonenhanced attenuation of greater than 10 HU, a feature that helps differentiate them from the much more common ACA (85). At contrast-enhanced CT, ACCs demonstrate heterogeneous enhancement with a peripheral predominance (84) (Fig 18). Areas of cystic change or necrosis are common, especially centrally. Intratumoral calcifications are seen in about 30% of cases (86) (Fig 18). Nonadenomatous lesions, including ACC, demonstrate slower relative and absolute washout than ACAs, with values of <40% and <60% at 15 minutes, respectively (16). Tumor thrombus in the renal vein and IVC is common. Local invasion, regional and paraaortic lymphadenopathy, and distant metastases to the lungs, liver, and bones are common at presentation (84).

The MR imaging appearance of ACC is characterized by low T1 signal and heterogeneously high T2 signal. Areas of hemorrhage may appear T1 hyperintense within the overall T1 hypointensity of the mass (84). Occasionally, ACC can contain small regions that lose signal on out-of-phase images (87). Although this feature is more commonly seen with ACAs, the overall aggressive heterogeneous appearance of ACC should help distinguish it from ACA. As with CT, contrast-enhanced MR imaging demonstrates a heterogeneous enhancement pattern with slow washout. MR imaging is particularly useful for assessing the renal vein and inferior ven cava for tumor thrombosis (88).

At ^{18}F FDG PET, ACC are hypermetabolic. ^{18}F FDG PET allows differentiation of ACC from ACA with a sensitivity of 100% and specificity of 88% using an adrenal-to-liver max SUV (standardized uptake value) ratio of 1.45 (89). FDG PET is particularly useful for detecting metastatic disease.

Teaching Point

Multiple factors are helpful in distinguishing ACC from other adrenal neoplasms. Most important, a heterogeneous enhancing adrenal mass greater than 4 cm in diameter has a high likelihood of malignancy, with approximately 70% of ACCs measuring >6 cm (84,90). Both CT and MR imaging can be useful to diagnose benign conditions that can mimic ACC. An adrenal mass measuring <10 HU at nonenhanced CT or with >40% or >60% relative and absolute washout rates, respectively, is most consistent with an ACA. The presence of regions of intralesional bulk fat is highly suggestive of an adrenal myelolipoma, although rare reports of ACC containing fat are present in the literature (91) (Fig 18).

Treatment depends on the extent of disease but typically is surgical followed by chemoradiotherapy. Despite advances in diagnosis and treatment, ACC continues to have a poor prognosis. Early diagnosis with primary resection is required for cure. The overall 5-year survival rate is poor (37%) (92).

Lymphoma

Primary lymphoma in the adrenal is extremely rare. Lymphoma is categorized as primary if it is confined to a single organ and immediately adjacent lymph nodes; otherwise, the lymphoma is considered secondary (93) (Fig 19). Secondary involvement of the adrenals by lymphoma is much more common and has been reported in up to 25% of patients with advanced disease at autopsy (94).

Lymphomatous involvement of the adrenals can occur in focal, multifocal, or diffuse patterns. Discrete solid nodules are seen in the focal and multifocal patterns. Diffuse involvement manifests as uniform organ infiltration often leading to enlargement (93). When discrete nodules are seen, the nodules tend to be well-demarcated, round, homogeneous, and demonstrate mild enhancement (93) (Fig 19). Calcification is uncommon unless there has been prior treatment. Adrenal lymphoma is bilateral in approximately 50% of cases (95) (Fig 19). The differential diagnosis of the focal nodular pattern of disease would include ACA, pheochromocytoma, ACC, and solitary metastasis. With the multifocal pattern, the main mimic would be metastatic disease. In the diffuse form, adrenal hyperplasia would be a consideration.

Sonographically, primary adrenal lymphoma has been described as a solid mass with variable echogenicity and cystic change (96). This is likely due to varying degrees of hemorrhage and necrosis, as described in a recent review of cases reported to date, confirming the predominant pattern as heterogeneously hypoechoic, with no reported cases being described as homogeneously hyperechoic (97).

A variety of CT appearances of primary adrenal lymphomas have been reported. A recent review of the CT appearance of 45 primary adrenal lymphomas described an approximately even distribution of homogeneous and heterogeneous patterns, with the majority of tumors having a hypoattenuating appearance and slight to moderate enhancement (97). In secondary adrenal lymphoma, the adrenals may appear normal, diffusely enlarge while maintaining a normal morphology, or demonstrate solitary or multiple masses (98) (Fig 20). Extensive retroperitoneal disease may engulf the adrenal. Secondary lymphoma tends to be homogeneous in attenuation with low-level enhancement and slow washout on delayed images. Calcifications are rare in the absence of prior treatment (99).

At MR imaging, primary and secondary lymphomas are hypointense to isointense on T1-weighted images and hyperintense on T2-weighted images when compared with liver (98).

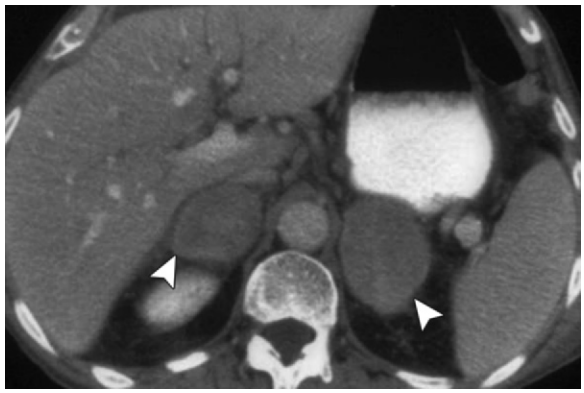

Figure 19. Adrenal lymphomas in a 77-year-old man with previous large B-cell lymphoma. Axial postcontrast CT image shows bilateral well-circumscribed hypoattenuating adrenal masses (arrowheads), later confirmed to represent secondary involvement.

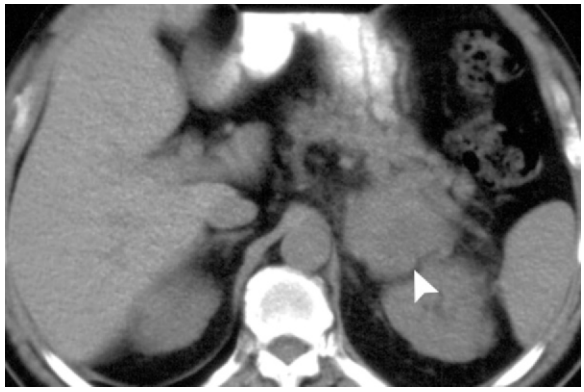

Figure 20. Adrenal lymphoma in a 57-year-old man. Axial CT image shows a solitary homogeneously hypoattenuating left adrenal mass (arrowhead), consistent with known recurrence of lymphoma.

Mild to moderate enhancement is commonly seen (100). Given the highly cellular nature of lymphomatous masses, restricted diffusion is commonly seen (97). ^{18}F FDG PET is commonly performed for staging and treatment monitoring in lymphoma and may be helpful in evaluation of the adrenals (101).

Given the varied imaging patterns of disease that are possible with adrenal lymphoma, the imaging findings are rarely specific. If the adrenal mass(es) cannot be shown to contain visible regions of fat, as in myelolipoma, or to represent an ACA at adrenal protocol CT or chemical shift MR imaging, then lymphoma remains a possibility, along with other benign and malignant conditions. With diffuse gland involvement, adrenal hyperplasia should be considered. The presence of aggressive vascular invasion would suggest ACC rather than lymphoma, which tends to surround vessels rather than displace them. The presence of calcifications in a large adrenal lesion that has

Figure 21. Adrenal leiomyosarcoma in a 75-year-old woman with abdominal tenderness. Axial postcontrast CT image shows a heterogeneous solid and cystic leiomyosarcoma (arrowhead), which invaded the adrenal and renal capsule.

not been treated would suggest ACC rather than lymphoma. If results of clinical and laboratory analysis are inconclusive, then tissue sampling is often needed for definitive diagnosis. In the setting of known lymphoma, the diagnosis may be presumed, with imaging follow-up to assess for treatment response.

Clinical management is initial treatment with chemotherapy or combined-modality therapy followed by restaging at completion of chemotherapy to assess treatment response.

Sarcoma

Sarcomas primary in the adrenal are rare; two tumors that may occur include angiosarcoma and leiomyosarcoma. Angiosarcoma is a rare mesenchymal tumor originating within the adrenal. Leiomyosarcoma arises from the adrenal vein smooth muscle or is associated with its tributaries in the gland. This is similar to leiomyosarcoma originating elsewhere in the retroperitoneum, such as the IVC.

Confident diagnosis of an angiosarcoma can be made when the tumor has a vasoformative pattern, but can be more challenging when an epithelioid more solid pattern exists. Endothelial differentiation can be confirmed with positivity for factor VIII–related antigen, CD31, CD34, or ERG transcription factor (7).

Both angiosarcoma and leiomyosarcoma are typically large and heterogeneous in appearance with an irregular margin at CT and may have calcifications internally (102) (Fig 21). Leiomyosarcomas demonstrated decreased signal intensity on T1-weighted images and increased signal intensity on T2-weighted images with marginal enhancement (103). Large ACAs with hemorrhage centrally may mimic an angiosarcoma. ACC and other malignancies are also in the differential diagnosis, given the heterogeneity and calcifications that can occur in adrenal sarcomas, typically leading to excision if possible.

Metastases

Commonly, radiologists are asked to exclude adrenal metastases in patients with known extra-adrenal primary neoplasms. The true prevalence of these secondary tumors to the adrenal is debated and likely varies according to practice and patient population. However, the literature suggests that the rate of malignant tumors occurring within the total number of incidentally identified adrenal masses is near 2%–3% and may be as high as 30% in practices with an oncologic emphasis (104). In addition, a history or the presence of an extra-adrenal malignancy in a patient increases the risk that an unanticipated adrenal mass identified at imaging will be malignant (104). Adrenal metastases were confirmed in 27% of autopsy examinations in a series of patients with extra-adrenal malignant epithelial tumors (105). The most common tumors to metastasize to the adrenal are carcinomas (lung, breast, and colon), malignant melanoma, and lymphoma (104) (Fig 22).

Unfortunately, the imaging appearance of many of these tumors is nonspecific. A bilateral distribution is more common than unilateral involvement, but any new adrenal mass should be considered metastatic involvement until proven otherwise in a patient with a known primary malignancy elsewhere (Fig 22). The presence of intratumoral lipid or fat may be helpful in determining that a lesion represents an ACA or myelolipoma rather than a metastasis, using techniques previously discussed. However, care should be taken to consider the possibility of a metastasis to a preexisting lesion (eg, a collision tumor between a metastasis and an ACA or myelolipoma).

In patients with a known primary malignancy elsewhere, lesions >3 cm tend to be metastases (106). At nonenhanced CT, an adrenal metastasis should be suspected when a noncalcified, nonhemorrhagic mass demonstrates attenuation values 43 HU (106). At MR imaging, adrenal metastases demonstrate low T1 signal and increased T2 signal with progressive enhancement (18). Ultimately, in a patient with a known malignancy, metastases should be considered unless a definitive diagnosis of a benign lesion can be made.

Approach to Adrenal Tumors

Adrenal tumors are common and can be broadly grouped into lesions that are either benign or malignant and either hormonally active or inactive. The imager's role is to assess a lesion's anatomic and physiologic features to differentiate the likely

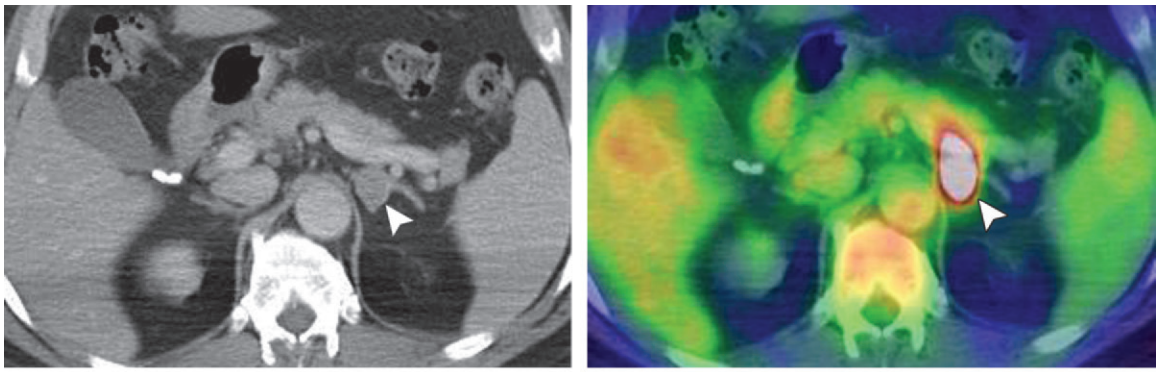

a. b.

Figure 22. Adrenal metastasis in a 61-year-old man with known cutaneous melanoma. **(a)** Axial postcontrast CT image shows a left adrenal nodule (arrowhead) that is nonspecific in appearance, resulting in an indeterminate classification and leading to further assessment. **(b)** Axial PET/CT image shows markedly increased metabolic activity (arrowhead), which was shown to represent a melanoma metastasis.

benign from the likely malignant. Key features include size, internal characteristics (eg, necrosis), enhancement, washout features, isotope avidity, and findings of local, regional, and distant metastatic disease.

The vast majority of benign adrenal tumors are ACAs containing varying amounts of intracytoplasmic lipid. These ACAs can be diagnosed based on the combination of findings of a homogeneous small lesion, usually measuring 4 cm or smaller, with a nonenhanced CT value of <10 HU. The less common lipid-poor ACAs rely on absolute or relative washout percentages >60% and >40%, respectively, or chemical shift MR imaging with loss of signal intensity on the out-of-phase image. Myelolipomas are benign lesions that contain macroscopic levels of grossly visible fat detectable with both CT and MR imaging with fat saturation techniques. Rarely, the diagnosis is complicated by a collision tumor, which consists of independently coexisting tumors within the same mass (such as a metastasis occurring within an ACA, or less commonly within a myelolipoma).

Hypervascular tumors between 3 and 5 cm that contain T2 bright components are highly suspicious for pheochromocytoma. The diagnosis is substantiated with nuclear medicine agents such as MIBG, which simultaneously confirm the origin of the tumor while assessing for both multifocal and metastatic disease. Infrequently, pheochromocytomas have imaging features more suggestive of an ACA. An increasing number of unanticipated pheochromocytomas are being identified in patients undergoing imaging for other reasons, many of which are without adrenal hyperfunction.

Large tumors measuring ≥6 cm are highly suspicious for malignancy, including ACCs. Other than nonoperative lesions such as hematoma, the majority of these are excised.

Bilateral lesions may suggest either a benign or malignant process, as may be seen in hemorrhage, ACH, infection, lymphoma, or metastases. Clinical history (eg, history of trauma or bleeding diathesis), size of the lesions (eg, size >3 cm more likely to represent metastases), and secondary imaging findings can be helpful in suggesting the diagnosis (eg, retroperitoneal lymphadenopathy as may be seen in lymphoma).

The presence of calcification is similarly seen in both benign and malignant tumors. If calcifications are present in a large mass, then ACC should be strongly considered. Calcifications may also be seen in smaller masses as the sequel of previous hemorrhage or granulomatous disease and can be seen in degenerating ACAs or infrequently in pheochromocytoma (5%–10% of cases). Bilaterality of calcification may be helpful in suggesting a benign etiology.

Before any surgical procedure, as well as before percutaneous image-guided biopsy, it is imperative that all patients be screened for catecholamine excess so that these cases can be pharmacologically blocked. Furthermore, the laterality of a hormonally active lesion may need to be confirmed with venous sampling before its excision to ensure the appropriate side is removed.

Conclusion

Radiologists play an important role in identification and diagnosis of tumors and tumor-like conditions in the symptomatic and asymptomatic patient. More specifically, the astute radiologist can categorize those lesions as benign or malignant based on the imaging findings that have been established previously via radiologic-pathologic correlation. Radiologists will continue to play an important role in the diagnostic process in conjunction with the primary care provider, surgeon, and pathologist.

Acknowledgment.—We greatly appreciate the assistance of Brent Wagner, MD, who served as a radiology consultant and provided editorial support. Special thanks to Gilbert Gardner, MA, CMI, for the medical illustration.

References

1. Blake MA, Cronin CG, Boland GW. Adrenal imaging. AJR Am J Roentgenol 2010;194(6):1450–1460.
2. Arnold DT, Reed JB, Burt K. Evaluation and management of the incidental adrenal mass. Proc (Bayl Univ Med Cent) 2003;16(1):7–12.
3. Terzolo M, Stigliano A, Chiodini I, et al. AME position statement on adrenal incidentaloma. Eur J Endocrinol 2011;164(6):851–870.
4. Berland LL, Silverman SG, Gore RM, et al. Managing incidental findings on abdominal CT: white paper of the ACR incidental findings committee. J Am Coll Radiol 2010;7(10):754–773.
5. Cawood TJ, Hunt PJ, O'Shea D, Cole D, Soule S. Recommended evaluation of adrenal incidentalomas is costly, has high false-positive rates and confers a risk of fatal cancer that is similar to the risk of the adrenal lesion becoming malignant; time for a rethink? Eur J Endocrinol 2009;161(4):513–527.
6. Young WF. Primary aldosteronism: renaissance of a syndrome. Clin Endocrinol (Oxf) 2007;66(5):607–618.
7. Lack EE. Tumors of the adrenal glands and extraadrenal paraganglia. Series 4, fascicle 8. Washington, DC: American Registry of Pathology, 2007; 1–297.
8. Mayo-Smith WW, Boland GW, Noto RB, Lee MJ. State-of-the-art adrenal imaging. RadioGraphics 2001;21(4):995–1012.
9. Motta-Ramirez GA, Remer EM, Herts BR, Gill IS, Hamrahian AH. Comparison of CT findings in symptomatic and incidentally discovered pheochromocytomas. AJR Am J Roentgenol 2005;185(3):684–688.
10. Kloos RT, Gross MD, Francis IR, Korobkin M, Shapiro B. Incidentally discovered adrenal masses. Endocr Rev 1995;16(4):460–484.
11. Lloyd RV, Tischler AS, Kimura N, McNicol AM, Young WF Jr. Tumours of the adrenal gland. In: DeLellis RA, Lloyd RV, Heitz PU, Eng C, eds. World Health Organization classification of tumours: pathology and genetics of tumours of endocrine organs. Lyon, France: IARC Press, 2004; 137–147.
12. Abrams HL, Siegelman SS, Adams DF, et al. Computed tomography versus ultrasound of the adrenal gland: a prospective study. Radiology 1982;143(1):121–128.
13. Johnson PT, Horton KM, Fishman EK. Adrenal mass imaging with multidetector CT: pathologic conditions, pearls, and pitfalls. RadioGraphics 2009;29(5):1333–1351.
14. Lee MJ, Hahn PF, Papanicolaou N, et al. Benign and malignant adrenal masses: CT distinction with attenuation coefficients, size, and observer analysis. Radiology 1991;179(2):415–418.
15. Johnson PT, Horton KM, Fishman EK. Adrenal imaging with multidetector CT: evidence-based protocol optimization and interpretative practice. RadioGraphics 2009;29(5):1319–1331.
16. Korobkin M, Brodeur FJ, Francis IR, Quint LE, Dunnick NR, Londy F. CT time-attenuation washout curves of adrenal adenomas and nonadenomas. AJR Am J Roentgenol 1998;170(3):747–752.
17. Korobkin M, Giordano TJ, Brodeur FJ, et al. Adrenal adenomas: relationship between histologic lipid and CT and MR findings. Radiology 1996;200(3):743–747.
18. Elsayes KM, Mukundan G, Narra VR, et al. Adrenal masses: MR imaging features with pathologic correlation. RadioGraphics 2004;24(suppl 1):S73–S86.
19. Patel J, Davenport MS, Cohan RH, Caoili EM. Can established CT attenuation and washout criteria for adrenal adenoma accurately exclude pheochromocytoma? AJR Am J Roentgenol 2013;201(1):122–127.
20. Russell RP, Masi AT. The prevalence of adrenal cortical hyperplasia at autopsy and its association with hypertension. Ann Intern Med 1970;73(2):195–205.
21. Dobbie JW. Adrenocortical nodular hyperplasia: the ageing adrenal. J Pathol 1969;99(1):1–18.
22. Lockhart ME, Smith JK, Kenney PJ. Imaging of adrenal masses. Eur J Radiol 2002;41(2):95–112.
23. Sohaib SA, Hanson JA, Newell-Price JD, et al. CT appearance of the adrenal glands in adrenocorticotrophic hormone-dependent Cushing's syndrome. AJR Am J Roentgenol 1999;172(4):997–1002.
24. Kawashima A, Sandler CM, Ernst RD, et al. Imaging of nontraumatic hemorrhage of the adrenal gland. RadioGraphics 1999;19(4):949–963.
25. Rana AI, Kenney PJ, Lockhart ME, et al. Adrenal gland hematomas in trauma patients. Radiology 2004;230(3):669–675.
26. Sevitt S. Post-traumatic adrenal apoplexy. J Clin Pathol 1955;8(3):185–194.
27. Burks DW, Mirvis SE, Shanmuganathan K. Acute adrenal injury after blunt abdominal trauma: CT findings. AJR Am J Roentgenol 1992;158(3):503–507.
28. Xarli VP, Steele AA, Davis PJ, Buescher ES, Rios CN, Garcia-Bunuel R. Adrenal hemorrhage in the adult. Medicine (Baltimore) 1978;57(3):211–221.
29. Rosenberger LH, Smith PW, Sawyer RG, Hanks JB, Adams RB, Hedrick TL. Bilateral adrenal hemorrhage: the unrecognized cause of hemodynamic collapse associated with heparin-induced thrombocytopenia. Crit Care Med 2011;39(4):833–838.
30. Arnason JA, Graziano FM. Adrenal insufficiency in the antiphospholipid antibody syndrome. Semin Arthritis Rheum 1995;25(2):109–116.
31. Arlt W. The approach to the adult with newly diagnosed adrenal insufficiency. J Clin Endocrinol Metab 2009;94(4):1059–1067.
32. Carvounis E, Marinis A, Arkadopoulos N, Theodosopoulos T, Smyrniotis V. Vascular adrenal cysts: a brief review of the literature. Arch Pathol Lab Med 2006;130(11):1722–1724.
33. Incze JS, Lui PS, Merriam JC, Austen G, Widrich WC, Gerzof SG. Morphology and pathogenesis of adrenal cysts. Am J Pathol 1979;95(2):423–432.
34. Sanal HT, Kocaoglu M, Yildirim D, et al. Imaging features of benign adrenal cysts. Eur J Radiol 2006;60(3):465–469.
35. Ricci Z, Chernyak V, Hsu K, et al. Adrenal cysts: natural history by long-term imaging follow-up. AJR Am J Roentgenol 2013;201(5):1009–1016.
36. Polat P, Kantarci M, Alper F, Suma S, Koruyucu MB, Okur A. Hydatid disease from head to toe. RadioGraphics 2003;23(2):475–494.

37. Otal P, Escourrou G, Mazerolles C, et al. Imaging features of uncommon adrenal masses with histopathologic correlation. RadioGraphics 1999;19 (3):569–581.
38. Wedmid A, Palese M. Diagnosis and treatment of the adrenal cyst. Curr Urol Rep 2010;11(1):44–50.
39. Grumbach MM, Biller BM, Braunstein GD, et al. Management of the clinically inapparent adrenal mass ("incidentaloma"). Ann Intern Med 2003; 138(5):424–429.
40. Olsson CA, Krane RJ, Klugo RC, Selikowitz SM. Adrenal myelolipoma. Surgery 1973;73(5): 665–670.
41. Kenney PJ, Wagner BJ, Rao P, Heffess CS. Myelolipoma: CT and pathologic features. Radiology 1998;208(1):87–95.
42. Ioannidis O, Papaemmanouil S, Chatzopoulos S, et al. Giant bilateral symptomatic adrenal myelolipomas associated with congenital adrenal hyperplasia. Pathol Oncol Res 2011;17(3):775–778.
43. Kudva YC, Young WF Jr, Thompson GB, Grant CS, van Heerden JA. Adrenal incidentaloma: an important component of the clinical presentation spectrum of benign sporadic adrenal pheochromocytoma. Endocrinologist 1999;9(2):77–80.
44. Linnoila RI, Keiser HR, Steinberg SM, Lack EE. Histopathology of benign versus malignant sympathoadrenal paragangliomas: clinicopathologic study of 120 cases including unusual histologic features. Hum Pathol 1990;21(11):1168–1180.
45. Dluhy RG. Pheochromocytoma: death of an axiom. N Engl J Med 2002;346(19):1486–1488.
46. Nakamura E, Kaelin WG Jr. Recent insights into the molecular pathogenesis of pheochromocytoma and paraganglioma. Endocr Pathol 2006; 17(2):97–106.
47. de Krijger RR, van Nederveen FH, Korpershoek E, Dinjens WNM. New developments in the detection of the clinical behavior of pheochromocytomas and paragangliomas. Endocr Pathol 2006; 17(2):137–141.
48. Tischler AS. Molecular and cellular biology of pheochromocytomas and extra-adrenal paragangliomas. Endocr Pathol 2006;17(4):321–328.
49. Miyake H, Maeda H, Tashiro M, et al. CT of adrenal tumors: frequency and clinical significance of low-attenuation lesions. AJR Am J Roentgenol 1989;152(5):1005–1007.
50. Brink I, Hoegerle S, Klisch J, Bley TA. Imaging of pheochromocytoma and paraganglioma. Fam Cancer 2005;4(1):61–68.
51. Newhouse JH, Heffess CS, Wagner BJ, Imray TJ, Adair CF, Davidson AJ. Large degenerated adrenal adenomas: radiologic-pathologic correlation. Radiology 1999;210(2):385–391.
52. Colby GW, Banks KP, Torres E. AJR teaching file: incidental adrenal mass and hypertension. AJR Am J Roentgenol 2006;187(3 suppl):S470–S472.
53. Jacques AET, Sahdev A, Sandrasagara M, et al. Adrenal phaeochromocytoma: correlation of MRI appearances with histology and function. Eur Radiol 2008;18(12):2885–2892.
54. Varghese JC, Hahn PF, Papanicolaou N, Mayo-Smith WW, Gaa JA, Lee MJ. MR differentiation of phaeochromocytoma from other adrenal lesions based on qualitative analysis of T2 relaxation times. Clin Radiol 1997;52(8):603–606.
55. Blake MA, Kalra MK, Maher MM, et al. Pheochromocytoma: an imaging chameleon. RadioGraphics 2004;24(suppl 1):S87–S99.
56. Shapiro B, Copp JE, Sisson JC, Eyre PL, Wallis J, Beierwaltes WH. Iodine-131 metaiodobenzylguanidine for the locating of suspected pheochromocytoma: experience in 400 cases. J Nucl Med 1985; 26(6):576–585.
57. Shulkin BL, Thompson NW, Shapiro B, Francis IR, Sisson JC. Pheochromocytomas: imaging with 2-[fluorine-18]fluoro-2-deoxy-D-glucose PET. Radiology 1999;212(1):35–41.
58. Timmers HJ, Chen CC, Carrasquillo JA, et al. Comparison of 18F-fluoro-L-DOPA, 18F-fluorodeoxyglucose, and 18F-fluorodopamine PET and 123I-MIBG scintigraphy in the localization of pheochromocytoma and paraganglioma. J Clin Endocrinol Metab 2009;94(12):4757–4767.
59. Timmers HJ, Kozupa A, Chen CC, et al. Superiority of fluorodeoxyglucose positron emission tomography to other functional imaging techniques in the evaluation of metastatic SDHB-associated pheochromocytoma and paraganglioma. J Clin Oncol 2007;25(16):2262–2269.
60. Ilias I, Chen CC, Carrasquillo JA, et al. Comparison of 6-18F-fluorodopamine PET with 123I-metaiodobenzylguanidine and 111in-pentetreotide scintigraphy in localization of nonmetastatic and metastatic pheochromocytoma. J Nucl Med 2008;49(10):1613–1619.
61. Kawashima A, Sandler CM, Fishman EK, et al. Spectrum of CT findings in nonmalignant disease of the adrenal gland. RadioGraphics 1998;18(2):393–412.
62. Garcia M, Louis LB 4th, Vernon S. Cystic adrenal lymphangioma. Arch Pathol Lab Med 2004; 128(6):713–714.
63. Inokuchi T, Takiuchi H, Moriwaki Y, et al. Retroperitoneal ancient schwannoma presenting as an adrenal incidentaloma: CT and MR findings. Magn Reson Imaging 2006;24(10):1389–1393.
64. Guo YK, Yang ZG, Li Y, et al. Uncommon adrenal masses: CT and MRI features with histopathologic correlation. Eur J Radiol 2007;62(3): 359–370.
65. Maweja S, Materne R, Detrembleur N, et al. Adrenal ganglioneuroma. Am J Surg 2007;194(5): 683–684.
66. Radin R, David CL, Goldfarb H, Francis IR. Adrenal and extra-adrenal retroperitoneal ganglioneuroma: imaging findings in 13 adults. Radiology 1997;202(3):703–707.
67. El-Daly H, Rao P, Palazzo F, Gudi M. A rare entity of an unusual site: adenomatoid tumour of the adrenal gland: a case report and review of the literature. Pathol Res Int 2010;2010(2):702472.
68. Garg K, Lee P, Ro JY, Qu Z, Troncoso P, Ayala AG. Adenomatoid tumor of the adrenal gland: a clinicopathologic study of 3 cases. Ann Diagn Pathol 2005;9(1):11–15.
69. Liu YQ, Zhang HX, Wang GL, Ma LL, Huang Y. A giant cystic adenomatoid tumor of the adrenal gland: a case report. Chin Med J (Engl) 2010;123 (3):372–374.
70. Wong DD, Spagnolo DV, Bisceglia M, Havlat M, McCallum D, Platten MA. Oncocytic adrenocortical neoplasms: a clinicopathologic study of 13 new cases emphasizing the importance of their recognition. Hum Pathol 2011;42(4):489–499.
71. Tahar GT, Nejib KN, Sadok SS, Rachid LM. Adrenocortical oncocytoma: a case report and review of literature. J Pediatr Surg 2008;43(5): E1–E3.

72. Juliano JJ, Cody RL, Suh JH. Metastatic adrenocortical oncocytoma: a case report. Urol Oncol 2008;26(2):198–201.
73. Bisceglia M, Ludovico O, Di Mattia A, et al. Adrenocortical oncocytic tumors: report of 10 cases and review of the literature. Int J Surg Pathol 2004;12(3):231–243.
74. Kumar N, Singh S, Govil S. Adrenal histoplasmosis: clinical presentation and imaging features in nine cases. Abdom Imaging 2003;28(5):703–708.
75. Pulakhandam U, Dincsoy HP. Cytomegaloviral adrenalitis and adrenal insufficiency in AIDS. Am J Clin Pathol 1990;93(5):651–656.
76. Freda PU, Wardlaw SL, Brudney K, Goland RS. Primary adrenal insufficiency in patients with the acquired immunodeficiency syndrome: a report of five cases. J Clin Endocrinol Metab 1994;79 (6): 1540–1545.
77. Allolio B, Fassnacht M. Clinical review: adrenocortical carcinoma—clinical update. J Clin Endocrinol Metab 2006;91(6):2027–2037.
78. Wooten MD, King DK. Adrenal cortical carcinoma: epidemiology and treatment with mitotane and a review of the literature. Cancer 1993;72 (11):3145–3155.
79. Soon PS, McDonald KL, Robinson BG, Sidhu SB. Molecular markers and the pathogenesis of adrenocortical cancer. Oncologist 2008;13 (5):548–561.
80. Venkatesh S, Hickey RC, Sellin RV, Fernandez JF, Samaan NA. Adrenal cortical carcinoma. Cancer 1989;64(3):765–769.
81. King DR, Lack EE. Adrenal cortical carcinoma: a clinical and pathologic study of 49 cases. Cancer 1979;44(1):239–244.
82. Lau SK, Weiss LM. The Weiss system for evaluating adrenocortical neoplasms: 25 years later. Hum Pathol 2009;40(6):757–768.
83. Hamper UM, Fishman EK, Hartman DS, Roberts JL, Sanders RC. Primary adrenocortical carcinoma: sonographic evaluation with clinical and pathologic correlation in 26 patients. AJR Am J Roentgenol 1987;148(5):915–919.
84. Bharwani N, Rockall AG, Sahdev A, et al. Adrenocortical carcinoma: the range of appearances on CT and MRI. AJR Am J Roentgenol 2011;196(6):W706–W714.
85. Boland GW, Lee MJ, Gazelle GS, Halpern EF, McNicholas MM, Mueller PR. Characterization of adrenal masses using unenhanced CT: an analysis of the CT literature. AJR Am J Roentgenol 1998;171(1):201–204.
86. Fishman EK, Deutch BM, Hartman DS, Goldman SM, Zerhouni EA, Siegelman SS. Primary adrenocortical carcinoma: CT evaluation with clinical correlation. AJR Am J Roentgenol 1987; 148(3):531–535.
87. Ferrozzi F, Bova D. CT and MR demonstration of fat within an adrenal cortical carcinoma. Abdom Imaging 1995;20(3):272–274.
88. Soler R, Rodríguez E, López MF, Marini M. MR imaging in inferior vena cava thrombosis. Eur J Radiol 1995;19(2):101–107.
89. Groussin L, Bonardel G, Silvéra S, et al. 18F-fluorodeoxyglucose positron emission tomography for the diagnosis of adrenocortical tumors: a prospective study in 77 operated patients. J Clin Endocrinol Metab 2009;94(5):1713–1722.
90. Hussain S, Belldegrun A, Seltzer SE, Richie JP, Gittes RF, Abrams HL. Differentiation of malignant from benign adrenal masses: predictive indices on computed tomography. AJR Am J Roentgenol 1985;144(1):61–65.
91. Musante F, Derchi LE, Zappasodi F, et al. Myelolipoma of the adrenal gland: sonographic and CT features. AJR Am J Roentgenol 1988;151 (5):961–964.
92. Abiven G, Coste J, Groussin L, et al. Clinical and biological features in the prognosis of adrenocortical cancer: poor outcome of cortisol-secreting tumors in a series of 202 consecutive patients. J Clin Endocrinol Metab 2006;91(7):2650–2655.
93. Leite NP, Kased N, Hanna RF, et al. Cross-sectional imaging of extranodal involvement in abdominopelvic lymphoproliferative malignancies. RadioGraphics 2007;27(6):1613–1634.
94. Rosenberg SA, Diamond HD, Jaslowitz B, Craver LF. Lymphosarcoma: a review of 1269 cases. Medicine (Baltimore) 1961;40:31–84.
95. Anis M, Irshad A. Imaging of abdominal lymphoma. Radiol Clin North Am 2008;46(2): 265–285.
96. Vicks BS, Perusek M, Johnson J, Tio F. Primary adrenal lymphoma: CT and sonographic appearances. J Clin Ultrasound 1987;15(2):135–139.
97. Rashidi A, Fisher SI. Primary adrenal lymphoma: a systematic review. Ann Hematol 2013;92(12): 1583–1593.
98. Hussain HK, Korobkin M. MR imaging of the adrenal glands. Magn Reson Imaging Clin N Am 2004;12(3):515–544.
99. Sohaib SA, Reznek RH. Adrenal imaging. BJU Int 2000;86(suppl 1):95–110.
100. Zhou L, Peng W, Wang C, Liu X, Shen Y, Zhou K. Primary adrenal lymphoma: radiological, pathological, clinical correlation. Eur J Radiol 2012;81 (3):401–405.
101. Paes FM, Kalkanis DG, Sideras PA, Serafini AN. FDG PET/CT of extranodal involvement in non-Hodgkin lymphoma and Hodgkin disease. RadioGraphics 2010;30(1):269–291.
102. Ilias I, Sahdev A, Reznek RH, Grossman AB, Pacak K. The optimal imaging of adrenal tumours: a comparison of different methods. Endocr Relat Cancer 2007;14(3):587–599.
103. Lee CW, Tsang YM, Liu KL. Primary adrenal leiomyosarcoma. Abdom Imaging 2006;31(1): 123–124.
104. Boland GW, Blake MA, Hahn PF, Mayo-Smith WW. Incidental adrenal lesions: principles, techniques, and algorithms for imaging characterization. Radiology 2008;249(3):756–775.
105. Abrams HL, Spiro R, Goldstein N. Metastases in carcinoma; analysis of 1000 autopsied cases. Cancer 1950;3(1):74–85.
106. Chong S, Lee KS, Kim HY, et al. Integrated PET-CT for the characterization of adrenal gland lesions in cancer patients: diagnostic efficacy and interpretation pitfalls. RadioGraphics 2006;26(6): 1811–1824; discussion 1824–1826.

From the Radiologic Pathology Archives
Adrenal Tumors and Tumor-like Conditions in the Adult: Radiologic-Pathologic Correlation

Grant E. Lattin, Jr, MD • Eric D. Sturgill, MD • Charles A. Tujo, MD • Jamie Marko, MD • Katherine W. Sanchez-Maldonado, MS • William D. Craig, MD • Ernest E. Lack, MD

RadioGraphics 2014; 34:805–829 • **Published online** 10.1148/rg.343130127 • **Content Codes:** CT GU MR OI

Page 808
MR chemical shift imaging exploits the different precessional frequencies of protons in water versus protons in fat within the same voxel and creates in-phase and out-of-phase images in which signal from the protons is either additive or subtractive from one another. As with unenhanced CT, this sequence takes advantage of the abundant intracytoplasmic lipid found in the majority of ACAs. Most adenomas show a significant decrease in signal intensity on the out-of-phase images.

Page 811
Adrenal hemorrhage in the adult can be broadly divided into traumatic and nontraumatic causes, with the former accounting for the majority of cases. Traumatic adrenal hemorrhage is most commonly seen in the setting of blunt trauma, with multiple other coexistent visceral injuries often identified.

Page 815
Myelolipomas contain gross fat and are characteristically identified at CT based on the presence of macroscopic fat.

Page 817
Pheochromocytoma's broad range of imaging features has earned it the nickname "an imaging chameleon." Radiologists are reminded to include pheochromocytoma in the differential diagnosis of low-attenuation adrenal lesions, lesions with avid washout, and lesions with a dominant cystic component, depending on the clinical scenario and laboratory findings.

Page 823
Multiple factors are helpful in distinguishing ACC from other adrenal neoplasms. Most important, a heterogeneous enhancing adrenal mass greater than 4 cm in diameter has a high likelihood of malignancy, with approximately 70% of ACCs measuring >6 cm.